Evolution, 2023, **77(10)**, 2128–2143
https://doi.org/10.1093/evolut/qpad111
Advance access publication June 21, 2023
Original Article

Additive genetic and environmental variation interact to shape the dynamics of seasonal migration in a wild bird population

Paul Acker[1], Francis Daunt[2], Sarah Wanless[2], Sarah J. Burthe[2], Mark A. Newell[2], Michael P. Harris[2], Robert L. Swann[3], Carrie Gunn[2], Tim I. Morley[4], Jane M. Reid[1,4]

[1]Centre for Biodiversity Dynamics, Department of Biology, NTNU, Trondheim, Norway
[2]UK Centre for Ecology and Hydrology, Bush Estate, Penicuik, United Kingdom
[3]Highland Ringing Group, Tain, United Kingdom
[4]School of Biological Sciences, University of Aberdeen, Aberdeen, United Kingdom

Corresponding author: Paul Acker, Centre for Biodiversity Dynamics, Department of Biology, NTNU, 7491 Trondheim, Norway. Email: paul.acker@ntnu.no

Abstract

Dissecting joint micro-evolutionary and plastic responses to environmental perturbations requires quantifying interacting components of genetic and environmental variation underlying expression of key traits. This ambition is particularly challenging for phenotypically discrete traits where multiscale decompositions are required to reveal nonlinear transformations of underlying genetic and environmental variation into phenotypic variation, and when effects must be estimated from incomplete field observations. We devised a joint multistate capture–recapture and quantitative genetic animal model, and fitted this model to full-annual-cycle resighting data from partially-migratory European shags (*Gulosus aristotelis*) to estimate key components of genetic, environmental and phenotypic variance in the ecologically critical discrete trait of seasonal migration versus residence. We demonstrate non-negligible additive genetic variance in latent liability for migration, resulting in detectable micro-evolutionary responses following two episodes of strong survival selection. Further, liability-scale additive genetic effects interacted with substantial permanent individual and temporary environmental effects to generate complex nonadditive effects on expressed phenotypes, causing substantial intrinsic gene-by-environment interaction variance on the phenotypic scale. Our analyses therefore reveal how temporal dynamics of partial seasonal migration arise from combinations of instantaneous micro-evolution and within-individual phenotypic consistency, and highlight how intrinsic phenotypic plasticity could expose genetic variation underlying discrete traits to complex forms of selection.

Keywords: alternative tactics, capture–recapture animal model, cryptic genetic variation, gene by environment interaction, partial migration, quantitative genetic threshold trait

Teaser text

How do interacting genetic and environmental effects generate phenotypic variation in key traits that mediate population responses to environmental perturbations, and thereby shape complex eco-evolutionary dynamics? Answering such questions is fundamental to evolutionary biology but is highly challenging, especially for discrete traits expressed by free-living individuals. Here, genetic and environmental effects do not translate linearly into phenotypic variation, and inferences may be biased by nonrandom observation failure, causing intertwined challenges of conceptualization and estimation. This situation is epitomized by seasonal migration versus residence, a widespread trait that allows mobile animals to escape from circannual environmental perturbations, directly shaping spatio-seasonal population dynamics. Here, we fitted novel quantitative genetic capture-mark-recapture models to 12 years of individual-based data from a wild population of European shags. Our analyses demonstrate notable additive genetic and permanent individual variation in liability for migration, and show how these components combine to generate substantial gene-by-environment interaction variance in phenotypic expression of migration. We further show how these variance components underpinned trait dynamics through the study period, including rapid micro-evolutionary responses to selection. We thereby provide conceptual, analytical, and empirical advances that reveal the quantitative genetic basis for joint plastic and evolutionary rescue of partially migratory populations experiencing changing environments.

Introduction

Understanding population responses to environmental perturbations and changes, manifested through combinations of micro-evolution and plasticity, requires quantifying multiple components of variance underlying key traits, and disentangling their independent and interacting effects (Bay et al., 2017; Hansen & Pélabon, 2021; Kingsolver & Buckley, 2017; Sgrò et al., 2016). Specifically, the additive genetic variance defines the potential for micro-evolutionary responses to selection and hence for inherited cross-generational changes in phenotypic distributions. Together with permanent individual variance stemming from lifelong effects of developmental environments and/or nonadditive genetic effects, the additive genetic variance also shapes the degree of short-term phenotypic inertia due to repeatability, thereby generating potential for within-generation changes resulting from survival selection. Meanwhile, variance attributable to temporary effects of current environments

Received March 22, 2023; revisions received June 01, 2023; accepted June 08, 2023
Associate Editor: Ruth Shaw; Handling Editor: Tim Connallon

encompasses rapid phenotypic responses through labile plasticity. Quantifying these components, and pinpointing their joint effects on phenotypic dynamics, can therefore reveal how populations respond to environmental change over multiple timeframes (Bonnet et al., 2019; Gienapp et al., 2008; Merilä & Hendry, 2014; Pigeon et al., 2017). However, major conceptual and analytical advances, allowing estimation from wild population data, are still required to quantify and interpret complex effects and interactions that generate nonlinear constraints on phenotypic expression and micro-evolution (Chevin et al., 2022; Hansen & Pélabon, 2021; Morrissey, 2015).

Such challenges particularly concern traits that are expressed as discrete alternative states (e.g., movement vs. philopatry; breeding vs. nonbreeding; dormancy vs. activity; Caswell, 2001; Reid & Acker, 2022). Such traits are commonly shaped by numerous genetic and environmental effects, and hence appropriately treated within the framework of quantitative genetics. An explicit model is therefore needed for how linear combinations of effects generate nonlinear (dichotomous) phenotypic outcomes (i.e., nonlinear genotype–environment–phenotype map; Chevin et al., 2022; Houle et al., 2010). This is parsimoniously achieved by the long-standing threshold trait model (Gianola, 1982; Moorad & Promislow, 2011; Roff, 1996; Wright, 1934). Here, dichotomous alternative phenotypes are expressed when an underlying latent continuously distributed liability is above versus below some threshold (Figure 1A). Variances due to additive genetic, permanent individual, and temporary residual effects can be appropriately partitioned on the liability scale (de Villemereuil et al., 2016; Falconer & Mackay, 1996). However, phenotypic variation, on which selection acts, is structurally different because strictly additive effects on liabilities can generate nonadditive effects on the discrete phenotypes. Further, such nonadditive effects increase with distance of underlying liabilities from the threshold, causing intrinsic links between the liability mean and the phenotypic variance, thereby shaping emerging phenotypic plasticity (Figure 1; Dempster & Lerner, 1950; Reid & Acker, 2022).

Specifically, the threshold trait framework implies that phenotypic variation results from emerging interactions among underlying additive genetic, permanent individual, and temporary environmental effects. For example, the phenotypic effect of a particular allelic substitution will depend on the values of permanent and temporary environmental deviations. Hence, there can effectively be gene-by-environment interactions ("G × E") affecting the phenotype, even without any G × E on the liability scale (Figure 1; Reid & Acker, 2022). Comprehensive dissection of interacting genetic and environmental effects on discrete traits therefore requires explicit consideration of all components of liability-scale variance and their transformation into phenotypic variances (as initiated by de Villemereuil et al., 2016). Such multi-scale variance decompositions are now required to fully understand and predict joint plastic and micro-evolutionary responses to environmental perturbations and changes.

Such intrinsic conceptual complexities of discrete trait dynamics come hand-in-hand with challenges of estimation. Observed dichotomous phenotypes must be used to estimate latent liability-scale variances, which must then be back-transformed to derive phenotypic-scale variances. This is achievable using generalized linear mixed models ("GLMMs"), where a nonlinear data scale maps onto a linear latent scale through a link function (Nelder & Wedderburn, 1972). By incorporating pedigree data describing genealogical relationships among individuals, such models can explicitly estimate latent-scale additive genetic variances, forming "animal models" (de Villemereuil et al., 2016; Falconer & Mackay, 1996). Dynamics of latent liabilities and resulting phenotypes within and across years and generations

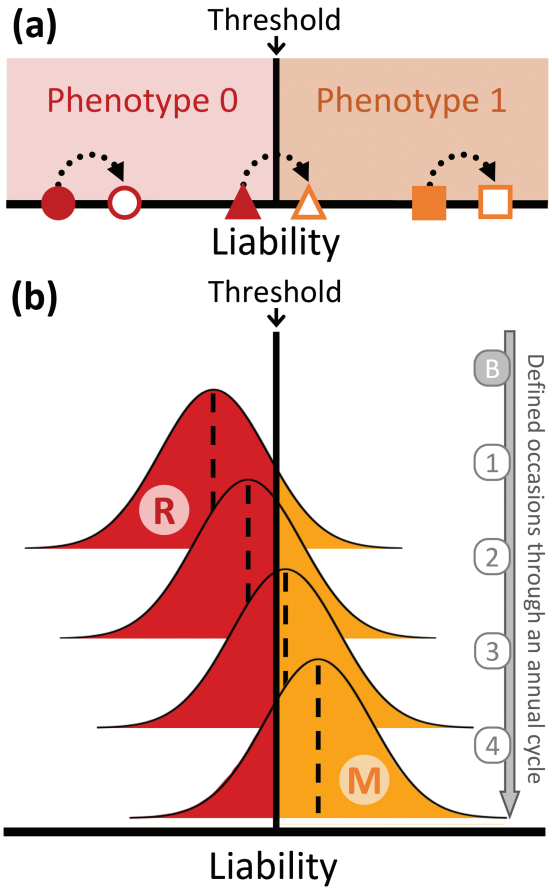

Figure 1. Multiscale principles of threshold trait variation. (A) Phenotype 0 versus 1 is expressed when the underlying continuous liability (x-axis) is below versus above a certain threshold. Filled symbols (circle, triangle, square) illustrate three individual liability intercepts of differing distance and direction from the threshold, reflecting genetic, and/or permanent environmental effects. Open symbols represent current individual liabilities encompassing temporary environmental variation. Here, identical additive effects (dotted arrows) either do or do not cause within-individual phenotypic variation (the triangle individual is phenotypically plastic while the circle and square individuals are not), implying interactions between liability intercepts and temporary environments that generate among-individual variation in phenotypic plasticity. More generally, dotted arrows could represent any variation in liability (e.g., an allelic substitution), highlighting that any set of additive effects on the liability scale must interact to nonadditively generate a phenotype. (B) The distribution of liabilities can change through time, illustrated here as a steady increase in mean liability (dashed vertical line) through an annual cycle of phenotypic expression for the trait seasonal migration ("M") versus residence ("R"). In the breeding season ("B"), there is no expression of M (i.e., all individuals express R) and hence no liability is represented. The liability is defined and represented on discrete occasions 1–4 through the nonbreeding season. Changes in population mean on the liability scale generate changes in the phenotypic proportion of residents and migrants (areas below and above the threshold, respectively), and hence in both mean and variance on the phenotypic scale.

can then be estimated, allowing inference on how changing additive genetic and environmental effects on liabilities interactively translate into changing frequencies of dichotomous phenotypes.

Yet, further major challenges arise in the common situation where phenotypic data are nonrandomly missing from datasets, which can substantially bias quantitative genetic estimates unless the (imperfect) observation process is modeled (Hadfield, 2008; Nakagawa & Freckleton, 2008). This is in principle achievable using joint capture–recapture and animal models ("CRAMs"; Papaïx et al., 2010). But, to date, such models have only been developed for the specific case of estimating additive genetic variance in survival, with one illustrative example (Papaïx et al., 2010; Morrissey et al., 2014; de Villemereuil, 2018). Implementation of general CRAMs, allowing estimation of variances underlying expression of any trait given incomplete observation, will therefore substantially advance capabilities to dissect trait dynamics in nature.

A prime example of these complexities of conceptualization and estimation is seasonal migration versus residence, a critical trait that directly shapes population dynamic outcomes in mobile animals inhabiting seasonally varying environments. Here, expression of seasonal migration (hereafter "migration") can vary within populations, whereby some individuals remain resident at the breeding location yearround while other individuals migrate for all or part of the nonbreeding season before returning to breed. Resulting "partial migration" occurs in numerous taxa, spanning fish, mammals, amphibians, reptiles, and birds (Berg et al., 2019; Buchan et al., 2020; Chapman et al., 2012; Grayson et al., 2011). Such phenotypic variation determines individuals' seasonal locations and resulting exposure to heterogeneous environments, thereby directly affecting fitness, driving selection, and shaping spatio-seasonal population dynamics (Reid et al., 2018). Given a compound additive genetic and environmental basis, expression of migration could therefore mediate eco-evolutionary dynamics in seasonally varying environments.

Migration versus residence has long been conceptualized as a threshold trait (Berthold, 1988; Dodson et al., 2013; Pulido et al., 1996). Substantial evidence shows that expression of migration, and closely related traits such as maturation or anadromy in salmonids, is highly polygenic (Bossu et al., 2022; Lemopoulos et al., 2019; Pedersen et al., 2013; Sinclair-Waters et al., 2020) and environmentally dependent (affected by e.g., individual state, density, predation, weather, or food; Boyle et al., 2010; Brodersen et al., 2008; Eggeman et al., 2016; Grayson et al., 2011; Yackulic et al., 2017). Further, while migration is commonly highly repeatable in iteroparous adults (e.g., Kerr et al., 2009; Grist et al., 2014; Zúñiga et al., 2017; Sawyer et al., 2019; Lehnert et al., 2018), considerable individual plasticity is also evident. Individuals can switch between migration and residence between winters (e.g., Brodersen et al., 2014; Grayson et al., 2011; Hegemann et al., 2015; Xu et al., 2021) and within winters (representing late departure from or early return to breeding locations; Cagnacci et al., 2011; Fudickar et al., 2013; Reid et al., 2020). Such combinations of high repeatability and labile plasticity across nested timescales imply substantial variation in permanent environmental and/or genetic effects, and non-negligible temporary environmental effects. However, corresponding variances in liability for migration, and the degree to which such effects change through time and interactively translate into phenotypic change, have never been explicitly quantified in free-living natural populations. Consequently, we cannot yet predict micro-evolutionary responses of partially migratory populations to environmentally-induced selection, or evaluate the potential for evolutionary rescue through changing seasonal movement.

Progress requires phenotypic observations of migration versus residence in numerous individuals of known relatedness, within and across years and generations. While this can be achieved through large-scale field resightings of marked individuals, resulting datasets inevitably include heterogeneous detection failure due to spatiotemporal variation in observation effort and success (Acker et al., 2021b). CRAMs that can partition variation in liability for migration while accounting for imperfect observation are therefore required to reveal the potential for rapid spatio-seasonal eco-evolutionary dynamics.

Here, we first summarize a general CRAM that allows inference on liability-scale effects and variances for any dichotomous trait using individual capture–recapture histories. We then fit this CRAM to 12 years of large-scale yearround resighting data on individual migration versus residence, coupled with >30 years of pedigree data from a partially migratory European shag (*Gulosus aristotelis*) population. We draw three levels of inference. First, we estimate the components of liability-scale variance attributable to additive genetic, permanent individual and temporary residual effects, and thereby evaluate the underlying potential for micro-evolution of seasonal migration. Second, we estimate the components of phenotypic-scale variance resulting from the nonlinear genotype–environment–phenotype map intrinsic to the threshold trait model, thereby revealing how liability-scale genetic and environmental variances interact to generate observed phenotypic variance. Third, we estimate changes in population-level mean additive genetic values, liabilities and resulting phenotypic proportions of migrants versus residents within and across the 12-year study, thereby revealing the magnitude and basis of temporal dynamics of migration. Specifically, we examine the degree to which two known episodes of strong survival selection against residence induced by extreme climatic events ("ECEs"; Acker et al., 2021b) caused persistent versus transient change in liability for migration and resulting phenotypic expression, through immediate micro-evolution versus changing distributions of permanent individual effects. Overall, we provide new conceptual and empirical insights into how latent and expressed components of trait variation can shape micro-evolutionary and phenotypic responses in a critical trait, seasonal migration versus residence, and thereby reshape spatio-seasonal population dynamics following environmental perturbations.

Methods

General principles of the CRAM

Typically, on any single wild population survey, some individuals are unobserved and consequently their phenotype cannot be measured (Lebreton et al., 1992; Nakagawa & Freckleton, 2008). Sampling bias occurs when such observation failure is nonrandom with respect to phenotype (e.g., Biro & Dingemanse, 2009). Yet, indirect inference on missing phenotypic data can still be made by modeling phenotype-dependent observation failure alongside the biological process of phenotypic variation (Gimenez et al., 2008;

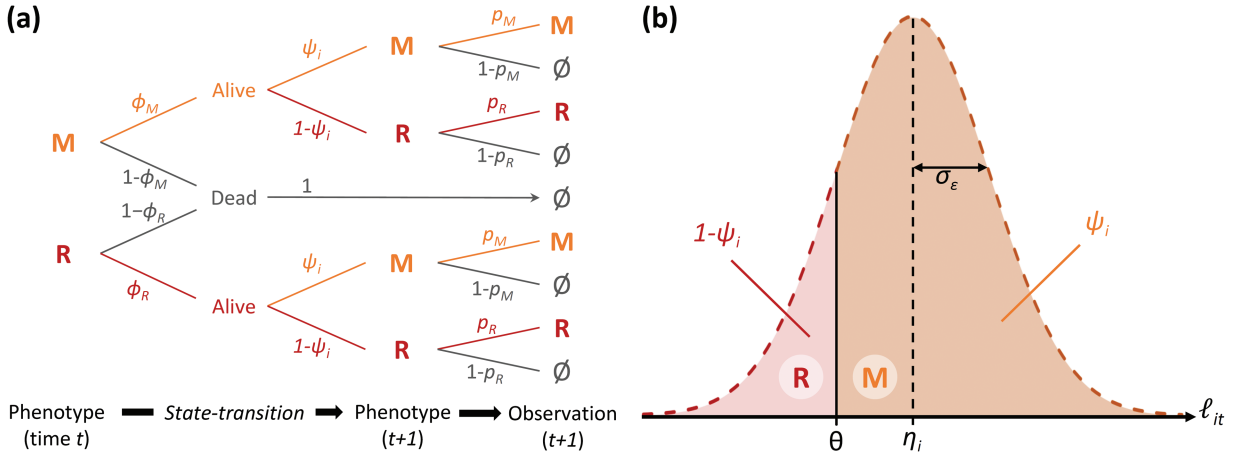

Figure 2. Discrete-time multistate capture–recapture model structure for a labile dichotomous threshold trait (e.g., seasonal migration versus residence). (A) Tree diagram summarizing the probabilistic formulation of all possible outcomes for individual i, comprising transitions between phenotypic states from time t to $t+1$, and observation at $t+1$. Between time points, the individual either survives or dies. On any time point, a surviving individual is in phenotypic state "migrant" (M) or "resident" (R) and can be resighted in its current state (observation M or R respectively) or not resighted (Ø). Dead individuals cannot be resighted. Indices on the branches indicate the probability of corresponding steps along the focal path: ϕ_M and ϕ_R for survival of migrants and residents, ψ_i for expressing phenotype M; p_M and p_R for resighting of migrants and residents. For illustration purposes, survival and resighting probabilities are here represented simply as phenotype-dependent, but can be time- and location-dependent. (B) Illustration of how the individual phenotypic expectation ψ_i relates to the distribution of the time-specific individual liability ℓ_{it}, assuming that ℓ_{it} is normally distributed with mean η_i and variance σ^2_ε. Under the threshold trait model, ψ_i is the probability that ℓ_{it} is greater than the threshold (θ). Accordingly, ψ_i is the area under the probability density function of ℓ_{it} between θ and $+\infty$, which is the value at θ of the cumulative distribution function of a standard normal of mean $\eta_i^* = \frac{\eta_i - \theta}{\sigma_\varepsilon}$. This is the probit transformation, $probit(\psi_i) = \eta_i^*$.

Nakagawa & Freckleton, 2008). Further, while instances of observation failure can be evident in longitudinal individual-based datasets if individuals reappear after previous absences, observation failure cannot be directly distinguished from death or permanent emigration (i.e., apparent mortality) after an individual is last encountered (Gimenez et al., 2008). Consequently, apparent mortality must also be modeled as part of the biological process that shapes true phenotypic variation. These objectives can be achieved using capture–recapture models, that is state-space models representing individual transitions between alive and dead states across time parameterized by survival probability ("ϕ"), and corresponding observations parameterized by detection probability ("p"; Gimenez et al., 2008; Lebreton et al., 1992). Further, different "alive" states can be defined to represent different phenotypes, with within-individual phenotypic variation parameterized by state-transition probabilities ("ψ") that are conditional on survival. This generates a multistate capture–recapture model (Lebreton & Pradel, 2002), which can be formulated to represent phenotypic variation in any discrete labile trait alongside phenotype-dependent survival and detection. The ambition now is to link individual variation in ψ (and/or ϕ) to a quantitative genetic animal model to form a CRAM (Papaïx et al., 2010; Morrissey et al., 2014; de Villemereuil, 2018), enabling estimation of components of (genetic) variance underlying phenotypic expression.

Nonrandom observation failure is inevitable when phenotypic data on migration versus residence are collected through field resightings of marked individuals in partially migratory populations (e.g., Grayson et al., 2011; Zúñiga et al., 2017), unless all potential nonbreeding season locations are similarly observed. To handle this scenario while estimating key components of underlying variance, we formulated a discrete-time multistate CRAM (Figure 2A). Here, the probability ψ_i that alive individual i transitions to the migrant phenotypic state ("M") corresponds to its probability of phenotype expression (i.e., its phenotypic expectation). Consequently, $1-\psi_i$ is the probability of expressing the resident phenotype ("R"; Figure 2A). Let z_{it} denote the phenotype of individual i at time t (assigning 0 for R and 1 for M), then:

$$z_{it} \sim Bernoulli(\psi_i), \quad (1)$$

$$E(z_{it}) = P(z_{it} = M) = \psi_i, \quad (2)$$

Under the threshold trait model, ψ_i is the probability that the underlying continuous liability ℓ_{it} exceeds the threshold θ. Assuming that ℓ_{it} is normally distributed with mean η_i and variance σ^2_ε (Figure 2B), as long-established in quantitative genetic theory (Wright, 1934; Dempster & Lerner, 1950; Falconer & Mackay, 1996; Supplementary Material S2):

$$\psi_i = P(\ell_{it} > \theta), \quad (3)$$

$$\ell_{it} \sim \mathcal{N}(\eta_i, \sigma^2_\varepsilon). \quad (4)$$

To decompose variance in liability for migration into additive genetic and other permanent and temporary components we define an animal model on ℓ_{it}, specified as a linear regression:

$$\ell_{it} = \mu + a_i + b_i + \varepsilon_{it}, \quad (5)$$

where $\mu + a_i + b_i = \eta_i$, μ is the overall mean, a_i is the additive genetic effect ("breeding value"; $\boldsymbol{a} \sim \mathcal{N}(0, \sigma^2_a \boldsymbol{A})$, where $\boldsymbol{a}$ is the vector of breeding values and $\boldsymbol{A}$ is the additive genetic relatedness matrix), b_i is the permanent individual effect (representing permanent environmental and nonadditive genetic effects; $b_i \sim \mathcal{N}(0, \sigma^2_b)$), and ε_{it} is the temporary residual (temporary individual effect encompassing labile plasticity; $\varepsilon_{it} \sim \mathcal{N}(0, \sigma^2_\varepsilon)$. However, this animal model is nonidentifiable because ℓ is a latent variable of unknown unit. Since θ is therefore also unknown, the link to phenotypic inference on ψ_i from the capture–recapture model cannot be made directly through equation (3). Yet, these problems can be circumvented by considering a standardized model, where liabilities

are threshold-centered and scaled by σ_ε (Dempster & Lerner, 1950):

$$\ell_{it}^{*} = \frac{\ell_{it} - \theta}{\sigma_\varepsilon}, \quad (6)$$

Standardized liability values ℓ_{it}^{*} are distances to the threshold and their unit is the standard deviation of the temporary residuals. This defines a reparametrized CRAM (equivalent to Equations 1 and 2) where the underlying variable is ℓ_{it}^{*}, the threshold is 0, and the residual variance is 1:

$$\psi_i = P\left(\ell_{it}^{*} > 0\right), \quad (7)$$

$$\ell_{it}^{*} \sim \mathcal{N}\left(\eta_i^{*}, 1\right), \quad (8)$$

$$\eta_i^{*} = \frac{\eta_i - \theta}{\sigma_\varepsilon}, \quad (9)$$

The phenotypic expectation ψ_i is therefore a simple function of η_i^{*}, specifically $\psi_{it} = F\left(\eta_i^{*}\right)$, where F is the cumulative distribution function of the standard normal distribution. Since F^{-1} is the probit function, we retrieve a binomial GLMM with a probit link (de Villemereuil et al., 2016; Supplementary Material S2):

$$probit\left(\psi_i\right) = \eta_i^{*} = \mu^{*} + a_i^{*} + b_i^{*}, \quad (10)$$

where $\mu^{*} = (\mu - \theta)/\sigma_\varepsilon$, $a_i^{*} = a_i/\sigma_\varepsilon$, and $b_i^{*} = b_i/\sigma_\varepsilon$.

Accordingly, we fit an identifiable animal model (Equation 10) on the probit-transformed individual phenotypic expectation inferred by the capture–recapture model, and hence formulate the joint likelihood of the multistate CRAM (Papaïx et al., 2010; Morrissey et al., 2014; de Villemereuil, 2018). It is critical to note that we estimate linear effects on the individual expectation η_i^{*} of the standardized liability for migration ℓ_{it}^{*}, centered on θ and scaled by σ_ε. Estimates of additive genetic and permanent individual variance in liability are therefore relative (σ_a^{*2} and σ_b^{*2}), and scaled by the temporary residual variance (i.e., $\sigma_a^{*2} = \sigma_a^2/\sigma_\varepsilon^2$, $\sigma_b^{*2} = \sigma_b^2/\sigma_\varepsilon^2$).

Study system and data collection

To quantify components of variance underlying migration versus residence using our CRAM, we collected observations of nonbreeding season locations of numerous pedigree-linked individuals in a partially-migratory shag population that breeds on Isle of May National Nature Reserve (hereafter "IoM"), Scotland (56°11′N, 2°33′W; Daunt et al., 2014; Frederiksen et al., 2008; Keogan et al., 2021). Banding and monitoring were licensed by British Trust for Ornithology and NatureScot.

During 1997–2021, ~20,600 chicks and ~1,100 adults were individually marked with a uniquely coded metal band and an inscribed color band field-readable from ~150 m with a telescope or camera. During nonbreeding seasons ("winters") 2009–2021, we collected resightings throughout September–February at coastal sites where individuals roost daily to dry their partially-wettable plumage (Grist et al., 2014; Acker et al., 2021b; Supplementary Material S1). We undertook ~ fortnightly surveys of main roost locations on IoM and across the population's migratory range in eastern Scotland, and obtained occasional resightings from other locations spanning ~800 km of coast. When an individual was resighted, we assigned its phenotype as resident (if seen on or near IoM) or migrant (if seen elsewhere; Supplementary Material S1).

During breeding seasons (April–June, "summers"), intensive monitoring of all nests and adjacent roost sites on IoM generated very high overall summer resighting probabilities of adults (0.90–0.98, mean 0.95 across 2010–2018; Acker et al., 2021a,b), including identification of most banded nest owners (~95% of all breeders in 2009–2021). Most adults (94%) were sexed through vocalizations and/or genotyping at a sex-linked marker (Acker et al., 2021b). Hence, since shags are socially monogamous, putative mothers, and/or fathers were assigned to banded chicks.

Previous phenotypic analyses in shags demonstrated structured patterns of among- and within-individual variation in migration versus residence that are consistent with expectations for a threshold trait, and inconsistent with simple Mendelian inheritance (Acker et al., 2023; Reid et al., 2020). This implies manifold genetic and/or environmental influences on migration, where quantitative genetic variance partitioning is appropriate for inferring micro-evolutionary and phenotypic dynamics.

Capture–recapture model design and resighting data set

To infer individual migration versus residence, we built the multistate capture–recapture part of the CRAM using a full-annual-cycle structure previously devised for estimating survival selection (Acker et al., 2021b). To maximize use of the field resightings, we divided each winter into four "occasions" when individuals can express phenotype M or R, and also included a summer occasion (Figures 1B and 2A). Although all individuals were assumed to be located on IoM in summer, and summer sightings provide no information on winter migration, utilizing the summer resightings facilitate precise inference on overall annual survival probabilities. This in turn facilitates inference on phenotypic variation and phenotype-dependent survival through intervening winters.

We defined six possible states that allowed us to represent the two phenotypes, M and R, while accounting for phenotype-dependent observation failure caused by spatio-temporal variation in resighting probability. Specifically, the migrant phenotype was represented by five states corresponding to four geographically distinct migratory areas with nonzero but potentially differing resighting effort, plus a "ghost area" representing all migrant destinations that were not surveyed (Acker et al., 2021b; Supplementary Material S1). The resident phenotype was represented by one state corresponding to the IoM area.

Individuals enter the dataset during the first summer they were observed to breed on IoM during 2009–2020. In summer, surviving individuals express phenotype R with probability 1. Between any two successive occasions across years, individuals either survive or die according to phenotype × sex × occasion × year-dependent ("×" denoting interactions) survival probability (ϕ). On each winter occasion, alive individuals express phenotype M or R according to probability ψ_i (where sources of variation are specified by the linear regression of probit(ψ_i) constituting the animal model part of the CRAM described below). Conditional on expressing phenotype M, individuals go to one of the five possible migrant areas. If an individual's phenotype was R in the previous occasion, it makes an initial move according to occasion × year × area-dependent destination probability δ (Supplementary Material S2). If the individual's phenotype was already M it can go to another migrant area according to movement

probability γ, which is low in our system, and hence was validly assumed constant across areas, occasions, and years (Acker et al., 2021b; Supplementary Material S2). Alive individuals can then be resighted where they are, and hence observed as M or R, or not resighted, according to sex × occasion × year × area-dependent resighting (detection) probability p (fixed to zero in the ghost area and for dead individuals; Supplementary Material S2).

We fitted this model to individual capture–recapture histories of 2,576 adult shags (1,319 females, 1,257 males) compiled from 61,281 year-round resightings (Supplementary Material S1). Each history comprises a sequence of observation events coding whether and in which area an individual was resighted, spanning all occasions until summer 2021. Each history ended with an additional final observation event indicating whether the individual was resighted again between summer 2021 and mid-December 2021. Including this last datum avoided parameter redundancy and allowed independent estimation of ϕ and p across all focal time steps through the 2009–2021 study period (Supplementary Material S2).

Animal model design and pedigree dataset

We formulated the animal model part of the CRAM by considering the standardized individual liability expectation η_i^*, that is the probit-transformed probability ψ_i of expressing phenotype M, thereby linking inference on trait variation with field observations analyzed by the capture–recapture part of the CRAM (see above). We allowed overall mean liability to differ among the four defined annual winter occasions, representing seasonal progression within each winter (e.g., Figure 1B). We also allowed mean liability to differ between sexes on each occasion. While current data are insufficient to estimate sex-specific additive genetic variance, modelling sex-specific means minimizes the risk that variance estimates are inflated by sexual dimorphism. Further, we kept the animal model relatively simple by modeling constant additive genetic and permanent environmental variances in liability for all winter occasions. This effectively assumes an across-occasion genetic correlation of 1 (e.g., Figure 1B). We therefore specified:

$$probit\left(\psi_{io}\right) = \eta_{io}^* = \mu_{os_i}^* + a_i^* + b_i^*, \tag{11}$$

where parameters are as in Equation 10, index s_i denotes the sex of individual i, and o denotes the winter occasion (nested within years; Supplementary Material S2). Any further variation in liability occurring across the whole range of environmental variation experienced by individuals throughout the study period (within and among years) was thus considered as random within individuals (ε_{it} on the liability scale), representing the temporary residual variance which gives the unit of the standardized liability scale. We also fitted additional models including effects of either brood, maternal, or paternal identity, to check whether shared developmental microenvironments caused resemblance among close kin that could have inflated estimates of σ_a^{*2}. However, these additional variance components were small, and estimates of σ_a^{*2} remained similar (Supplementary Material S2).

Beyond model design, pedigree-based quantitative genetic inference fundamentally depends on pedigree structure. To calculate the $\boldsymbol{A}$ matrix of pairwise correlations between individual breeding values a_i, we compiled pedigree data using observed social parentage of all phenotype-informative individuals (i.e., the 2,576 individuals in the capture-resighting dataset) and their ancestors (Supplementary Material S1). When same-brood individuals had an unbanded parent, they were assigned a common dummy parent, thereby linking known siblings (e.g., Husby et al., 2010). However, 20% of phenotype-informative individuals (518) were not known to be related to any other phenotype-informative individuals. Accordingly, they provide little information for estimating σ_a^{*2}, and attempts to estimate their breeding values a_i^* would be biased toward their phenotype which is also influenced by environmental effects (Hadfield et al., 2010; Postma, 2006). Hence, for these individuals, we replaced the animal model part of the CRAM with a simpler regression that did not distinguish additive genetic from permanent individual effects and instead simply considered their sum:

$$probit\left(\psi_{io}\right) = \mu_{os_i}^* + x_i^*, \tag{12}$$

where x_i^* is the total individual effect ($x_i^* \sim \mathcal{N}\left(0, \sigma_x^{*2}\right)$, $\sigma_x^{*2} = \sigma_a^{*2} + \sigma_b^{*2}$). Accordingly, the pedigree utilized to derive relatedness values informing estimation of σ_a^{*2} comprised 2,349 individuals, of which 88% (2,058) were phenotype-informative and 12% (291) were additional ancestors (including 86 dummy parents). Overall, 29% of these phenotype-informative individuals (602) and 90% of their additional ancestors (262) had both parents unknown and no siblings in the pedigree, comprising the defined founder population of (presumed) unrelated individuals for which σ_a^{*2} is estimated (Kruuk, 2004; Wolak & Reid, 2017). All other individuals (63% of the pedigree, 1,485 individuals) had both parents identified with known or dummy identities, hence achieving relatively high pedigree completeness (Wolak & Reid, 2017).

From this pedigree, we computed all pairwise additive genetic relatedness values (i.e., twice the expected coefficient of co-ancestry or kinship) between phenotype-informative individuals, that is the $\boldsymbol{A}$ matrix elements (Supplementary Material S1). There were 8,618 pairwise nonzero values: 18% ≤0.0625, 20% were 0.125, 31% were 0.25, and 31% were 0.5 (mean and median 0.25, standard deviation 0.17). Phenotype-informative individuals had a mean of 8.4 links with others (range 1–48, median 6, standard deviation 7.4). The per-individual mean of nonzero relatedness values was 0.35 (range 0.06–0.50, standard deviation 0.12) with a prominent mode at 0.5. Overall, this distribution demonstrates the existence of numerous close pedigree links, providing valuable information for estimating σ_a^{*2}.

Analyses of the multistate CRAM

We coded our CRAM in Stan, a probabilistic programming language for Bayesian inference, using package rstan (Carpenter et al., 2017) in R (R Core Team, 2022) to sample the posterior distribution of each parameter. For the capture–recapture model parameters, comprising probabilities, we used uniform priors (Supplementary Material S2). We retrieved estimates of survival, movement, and detection probabilities that were consistent with those obtained from our previous foundational model that did not include an animal model or estimate liability-scale parameters (Acker et al., 2021b). For the animal model parameters, we used weakly informative priors (Supplementary Material S2). A "control" CRAM, fitted after randomizing individual identities in the $\boldsymbol{A}$ matrix, showed no upward bias from the expected result of negligible σ_a^{*2} (Supplementary Material S2). Posterior predictive checks (Gelman et al., 1996) devised for the multistate

capture–recapture model (Acker et al., 2021b) indicated good overall fit. Details of posterior sampling procedures, diagnostics, and all parameter estimates are in Supplementary Material S4. Complete numerical summaries and posterior samples of all parameters are archived in Zenodo alongside Stan and R codes (see *Data accessibility statement*). Hereafter, estimates are presented as posterior means with 95% credible intervals ("95%CI").

Derived calculations

To achieve full liability-scale and phenotypic-scale variance decompositions for migration versus residence, we derived posterior distributions of compound and transformed quantities from the posterior samples of CRAM parameters. First, we extracted the total variance σ^{*2}_{ℓ} in liability on the standardized scale ($\sigma^{*2}_{\ell} = \sigma^{*2}_{a} + \sigma^{*2}_{b} + 1$, where 1 is the temporary residual variance $\sigma^{*2}_{e} = \sigma^{2}_{e}/\sigma^{2}_{e}$). We then calculated the proportions of total variance in liability (conditional on the fixed annual progression through winter occasions) attributable to total individual variance (i.e., repeatability, $\rho_{\ell} = \sigma^{*2}_{x}/\sigma^{*2}_{\ell}$) and to additive genetic variance (i.e., narrow-sense heritability, $h^{2}_{\ell} = \sigma^{*2}_{a}/\sigma^{*2}_{\ell}$.

Second, to quantify phenotypic-scale variation resulting from estimated liability-scale variation, we derived the overall phenotypic mean ($\bar{z}$) and phenotypic variance (V_z; where V denotes phenotypic-scale variances, while σ^2 denotes liability-scale variances). We then partitioned V_z into phenotypic-scale additive genetic variance (V_A) versus other components that involve permanent individual or temporary environmental variances (back-transformation formulae in Supplementary Material S3. Due to the general properties of mapping dichotomous traits to underlying continuous variables, the phenotypic mean and variance become interdependent (Figure 1B). Accordingly, our model implies occasion × sex-specific $\bar{z}$ and V_z (and its components). In addition, because some variation that is strictly additive on the liability-scale becomes nonadditive on the phenotypic-scale (Figure 1A; de Villemereuil et al., 2016; Dempster & Lerner, 1950), new components of phenotypic variance emerge from interactions between additive effects on the liability scale. More precisely, V_z is the sum of phenotypic variances resulting independently from liability-scale additive genetic effects, permanent individual effects, and temporary residual effects (V_a, V_b, and V_ε) plus phenotypic variances resulting from all possible interactions ($V_{a\times b}$, $V_{a\times\varepsilon}$, $V_{b\times\varepsilon}$, $V_{a\times b\times\varepsilon}$; Supplementary Material S3). Similarly, interactions between genes underpinning liability-scale additive genetic effects emerge on the phenotypic scale, implying that V_A is a subcomponent of V_a, alongside emerging nonadditive genetic variance V_{NA} (Dempster & Lerner, 1950; Robertson, 1950; de Villemereuil et al., 2016; Supplementary Material S3). From this decomposition, we further derived the phenotypic-scale total individual variance ($V_x = V_a + V_b + V_{a\times b}$), repeatability ($\rho_z = V_x/V_z$), and narrow-sense heritability ($h^2_z = V_A/V_z$).

Finally we derived estimates of population-level dynamics of breeding values, permanent individual values and overall liabilities for migration and resulting phenotypic expression through the 12 study years, thereby revealing micro-evolutionary and phenotypic changes in the adult population. Specifically, we derived the mean breeding value ($\bar{a}^*$), mean permanent individual effect ($\bar{b}^*$), mean standardized liability expectation ($\bar{\eta}^*$), and expected proportion of migrants ($\bar{\psi}$) for each occasion in each year (Supplementary Material S3). Here, temporal changes in $\bar{a}^*$ and $\bar{b}^*$ (and hence in $\bar{\eta}^*$ and $\bar{\psi}$) result from mortality of individuals already present in the focal adult population, and from entry of new individuals every summer. After their last sighting, the contributions of individuals to changes in $\bar{a}^*$. and $\bar{b}^*$ were inferred as functions of resighting and survival probabilities (Supplementary Material S3), which are phenotype-dependent in our CRAM Estimated changes in $\bar{a}^*$ and $\bar{b}^*$ thus partly rely on the assumption that individuals' current phenotypes are the sole cause of survival selection (Morrissey et al., 2010, 2012; Supplementary Material S3). Here, we focused on evaluating the evidence for changes ("Δ") in $\bar{a}^*$ or $\bar{b}^*$ between two consecutive time points surrounding the two known episodes of strong survival selection against residence (in late-winter 2012–2013 and 2017–2018; Acker et al., 2021b), and accordingly we did not explicitly quantify overall trends in $\bar{a}^*$ or $\bar{b}^*$ across the 12 years. Unlike in other studies (e.g., Biquet et al. , 2022; Bonnet et al., 2019; Gienapp et al., 2006; Hadfield et al., 2010; Hunter et al., 2022; Morrissey et al., 2012), the changes in $\bar{a}^*$ therefore substantially represent immediate micro-evolution resulting from selection among possible parents rather than changing breeding values across cohorts of offspring (Supplementary Material S3). We computed posterior distributions of Δ and calculated the probability "P_Δ" that Δ had the same sign as its posterior mean (Supplementary Material S3). $P_\Delta \approx 1$ indicates strong evidence for a positive or negative change, while $P_\Delta \approx 0.5$ indicates no clear evidence for either.

Results

Seasonal change in mean liability and phenotypic expression of migration

Our model retrieved expected patterns of seasonal change in mean liability for migration, and hence in phenotypic expression of migration versus residence (i.e., in overall phenotypic mean $\bar{z}$). Specifically, the overall liability-scale intercept μ was lowest and negative in September (winter occasion 1), then increased to values close to the threshold in October–February (winter occasions 2–4; Table 1, Figure 3). This general pattern was broadly similar in both sexes; μ was slightly lower in males than females in occasion 1, with no clear sex differences in occasions 2–4 (Table 1, Figure 3). Accordingly, the defined founder population was expected to contain more residents than migrants in September (occasion 1), particularly in males, and then similar proportions of the two phenotypes through the winter (i.e., occasions 2–4; Figure 3). The estimated liability-scale variation therefore implies substantial phenotypic-scale variation.

Liability-scale variance decomposition

The posterior distributions of the additive genetic variance (σ^{*2}_a) and permanent individual variance (σ^{*2}_b) in liability for migration (on the standardized liability scale) showed peaks of density that were clearly away from zero and hence distinct from the prior distributions (Figure 4). The magnitude of σ^{*2}_a was non-negligible, corresponding to approximately one third of the temporary residual variance (Figure 4A, Table 1), and demonstrating potential for micro-evolutionary change in liability for migration in response to selection. Meanwhile, σ^{*2}_b was notably large, corresponding to approximately three times the temporary residual variance (Figure 4B, Table 1). Consequently, there was very

Table 1. Capture–recapture animal model (CRAM) estimates of sex-specific occasion effects and variance components of the standardized liability underlying seasonal migration versus residence.

Parameter	Females	Males
Overall mean, occasion 1 ($\mu^*_{1,s}$)	–0.76 [–0.94, –0.58]	–1.31 [–1.52, –1.12]
Overall mean, occasion 2 ($\mu^*_{2,s}$)	–0.02 [–0.21, 0.17]	–0.15 [–0.33, 0.03]
Overall mean, occasion 3 ($\mu^*_{3,s}$)	0.04 [–0.16, 0.22]	0.09 [–0.09, 0.26]
Overall mean, occasion 4 ($\mu^*_{4,s}$)	–0.16 [–0.35, 0.02]	–0.20 [–0.37, –0.03]
Additive genetic variance (σ^{*2}_a)	0.41 [0.11, 0.77]	
Permanent individual variance (σ^{*2}_b)	2.87 [2.39, 3.40]	
Total individual variance (σ^{*2}_x)	3.28 [2.86, 3.75]	
Total trait variance (σ^{*2}_ℓ)	4.28 [3.86, 4.75]	
Repeatability (ρ_ℓ)	0.77 [0.74, 0.79]	
Heritability (h^2_ℓ)	0.09 [0.02, 0.18]	

Notes. The standardized liability scale is centered on the threshold (i.e., $\theta = 0$) and its unit is one standard deviation of the temporary residuals (i.e., $\sigma^{*2}_\varepsilon = 1$). The overall mean (i.e., common intercept for all individuals in the population) is specific to the within-winter occasion (1–4, representing mid-September to mid-October, mid-October to mid-November, mid-November to end December, and January to mid-February respectively; Supplementary Material S2) and sex (s), while the additive genetic variance and permanent individual variance are assumed constant across occasions and sexes. Estimates are given as the posterior mean and 95% credible intervals.

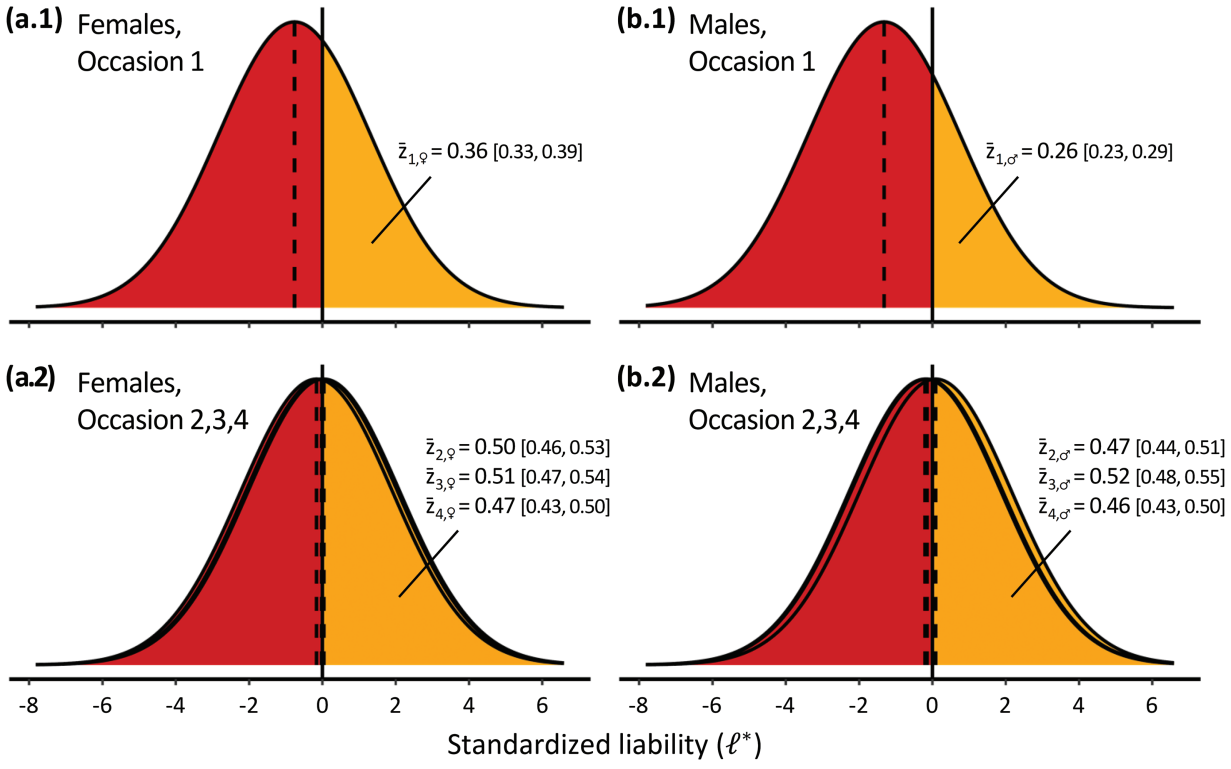

Figure 3. Density curves for occasion-specific distributions of the standardized liability for migration (ℓ) in (A, C) females and (B, D) males, for (A, B) seasonal occasion 1 (mid-September to mid-October) and (C, D) occasions 2–4 (spanning the rest of the winter), estimated from the capture–recapture animal model (CRAM). Dashed vertical lines represent distribution means (μ_{os} for any winter occasion o and sex s). Solid vertical lines represent the threshold (0 on the standardized liability scale). The area underneath the curve for $\ell^* > 0$ is the phenotypic mean $\bar{z}_{o,s}$, that is the expected proportion of migrants (and the area for $\ell^* < 0$ is the expected proportion of residents $1 - \bar{z}_{o,s}$). On c and d, curves for occasions 2–4 are superimposed because they are very similar. Numerical estimates of $\bar{z}_{o,s}$ are shown as posterior mean and 95% credible intervals. Numerical estimates for $\mu^*_{o,s}$ and σ^{*2}_x are in Table 1.

high liability-scale repeatability ($\rho_\ell \approx 77\%$), and modest liability-scale heritability ($h^2_\ell \approx 9\%$; Table 1).

Phenotypic-scale variance decomposition

Due to the large total variance in liability and proximity of the overall mean liability to the threshold, the total phenotypic in variance expression of migration versus residence V_z was always close to, or at, the maximum possible for a dichotomous trait (~0.2–0.25; Figure 5). Transformations of variance components from the liability scale to the phenotypic scale showed that the largest component of V_z was the variance coming from liability-scale permanent individual effects (b) independently of other effects (comprising ~47% of V_z; Figure 5). Meanwhile, the component of V_z coming purely from liability-scale additive genetic effects (a) was small, and essentially comprised phenotypic-scale additive genetic

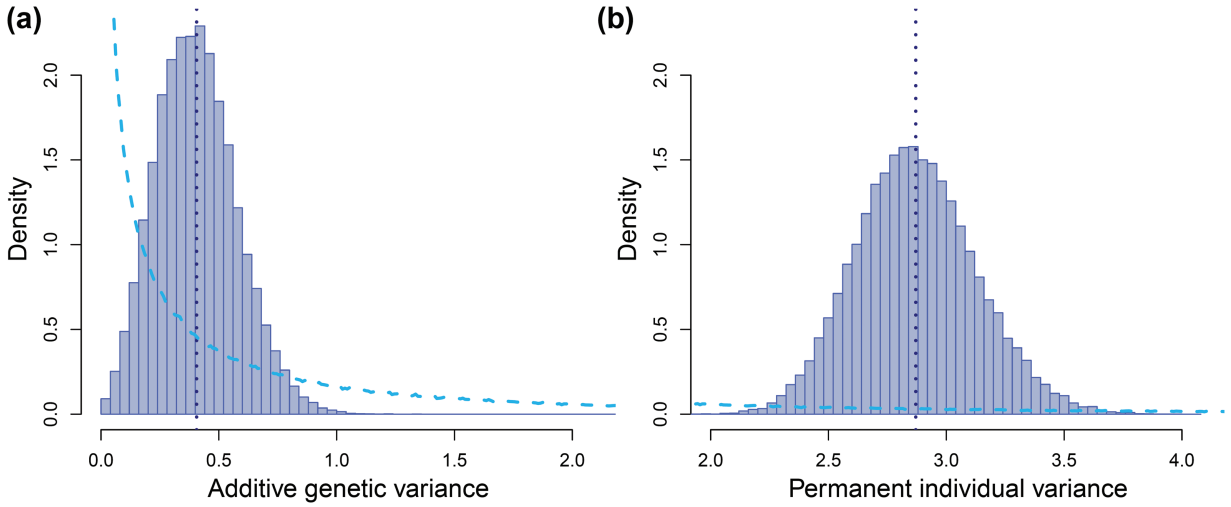

Figure 4. Prior (dashed line) and posterior (bars, MCMC samples) distributions of (A) additive genetic variance (σ^{*2}_a) and (B) permanent individual variance (σ^{*2}_b) in liability for seasonal migration versus residence. Dotted vertical lines indicate posterior means. Estimates are on the standardized liability scale, where the unit is one standard deviation of the temporary residuals of the liability (σ_ε).

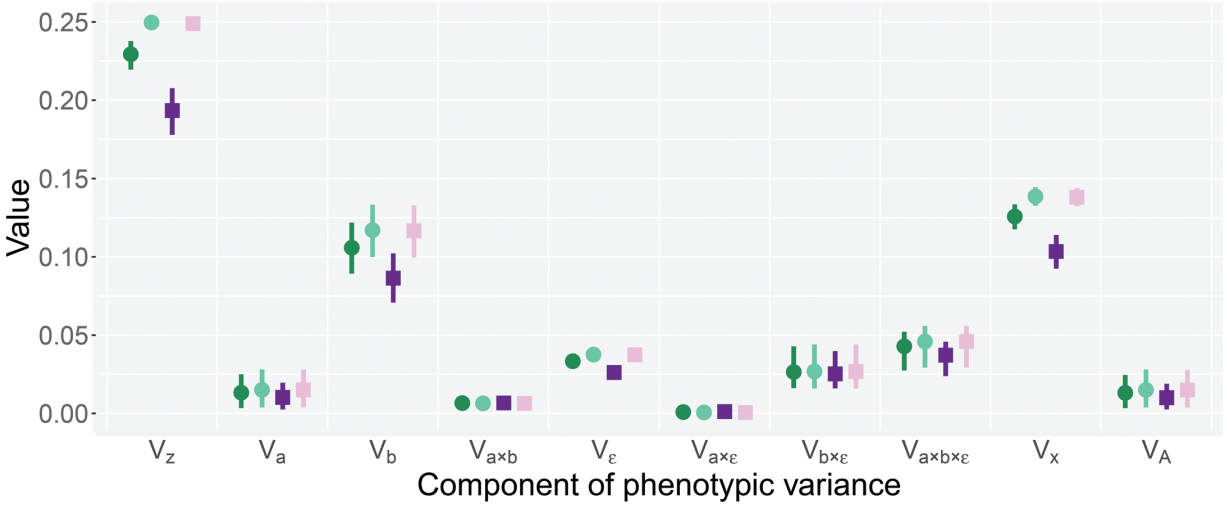

Figure 5. Decomposition of phenotypic variance (V_z) in seasonal migration versus residence, for females (circles) and males (squares) in winter occasion 1 (dark coloration, mid-September to mid-October) and occasion 2 (light coloration, mid-October to mid-November). Estimates for occasions 3 and 4 (spanning the rest of the winter) are virtually identical to occasion 2 (to two decimal places; Supplementary Material S3). V_z is the total phenotypic variance. V_a, V_b, and V_ε are the phenotypic variances arising independently from liability-scale additive genetic effects a, permanent individual effects b, and temporary residual effects ε, respectively. $V_{a\times b}$, $V_{a\times\varepsilon}$, $V_{b\times\varepsilon}$, and $V_{a\times b\times\varepsilon}$ are the phenotypic variances arising from interactions between these liability-scale effects. V_x is the total phenotypic-scale individual variance. V_A is the phenotypic-scale additive genetic variance. Point estimates are posterior means and lines indicate 95% credible intervals. Numerical details, including proportions of V_z, are in Supplementary Material S4.

variance (i.e., the emerging nonadditive genetic variance was negligible), yielding phenotypic-scale heritability h^2_z of ~6% (Figure 5) Furthermore, variance resulting from the emerging interaction between a and b constituted ~3% of V_z (Figure 5). Consequently, the high overall phenotypic repeatability of seasonal migration versus residence ($\rho_z \approx 55\%$; Figure 5) is primarily due to permanent individual rather than additive genetic effects.

Of the remaining 45% of V_z, constituting temporary phenotypic variance, approximately one third came purely from liability-scale temporary residual effects ε (comprising ~15% of V_z). The rest (comprising ~30% of V_z) came from nonadditive effects emerging from interactions between ε, a and b, encompassing among-individual variation in labile phenotypic plasticity (Figure 5). Here, the variance coming from $a \times \varepsilon$ was very small (≤1% of V_z), but those coming from $b \times \varepsilon$ and $a \times b \times \varepsilon$ were substantial (~11% and ~18%).

These outcomes were broadly similar for both sexes across all four defined winter occasions (Figure 5). The only notable quantitative difference was that the total phenotypic variance V_z was slightly lower in males than females in occasion 1 (Figure 5).

Population-level changes across the study period

Model predictions of population-level changes in liability and phenotypic expression of migration across the study period revealed multiscale responses to known episodes of strong ECE-induced survival selection. Mean breeding value in the adult population ($\bar{a}^*$) was stable across the first four years with posterior means slightly above the

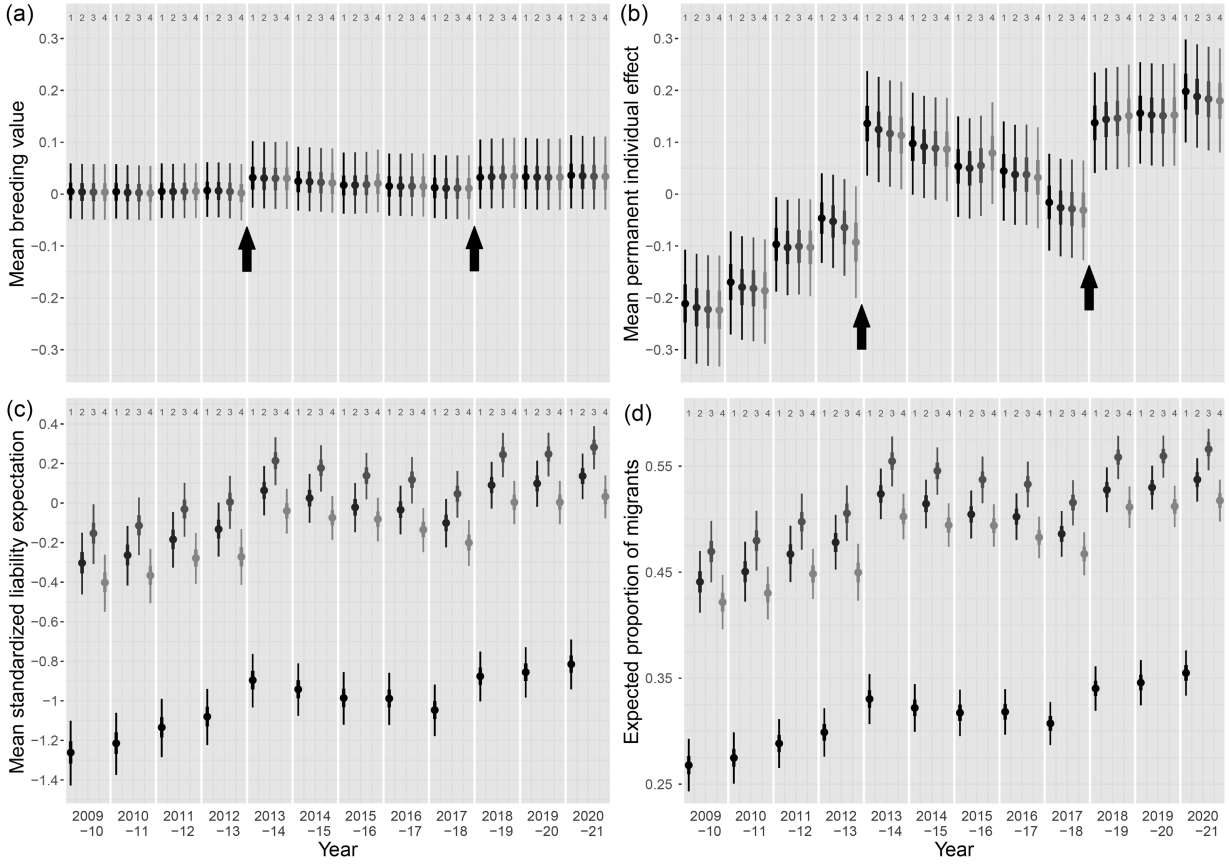

Figure 6. Estimated values of population means of (A) breeding values ($\bar{a}^*$), (B) permanent individual effects ($\bar{b}^*$), (C) standardized liability expectation ($\bar{\eta}^*$), and (D) expected proportion of migrants ($\bar{\psi}$), across the four defined occasions within each of the 12 focal biological years. The within-winter occasion (1–4) is indicated on top row and distinguishable across years by coloration shade (from black to light gray). Point estimates are posterior means, inner and outer line segments indicate 50% and 95% credible intervals. Black arrows on panels (A) and (B) point at the two episodes of strong survival selection that occurred in late-winter 2012–2013 and 2017–2018.

founder population mean of zero, then increased abruptly (to ~0.03 on the standardized liability scale) following the first known episode of strong selection against residence during late-winter 2012–2013 (Figure 6A). Subsequently, $\bar{a}^*$ progressively decreased (to ~0.01) until the next selection episode in late-winter 2017–2018, when it increased abruptly (to ~0.03), then remained stable across subsequent years (Figure 6A). There was high support for instantaneous increases in $\bar{a}^*$ following each selective ECE ($P_\Delta = 0.95$), indicating micro-evolutionary responses to selection.

The mean permanent individual effect $\bar{b}^*$ also increased dramatically following the two episodes of ECE-induced selection (Figure 6B, $P_\Delta = 1$), representing major shifts in the adult distribution of liabilities that are not heritable across generations. Further, $\bar{b}^*$ also varied between other consecutive years without strong survival selection (Figure 6B), largely reflecting variation in permanent individual effects among cohorts of recruiting adults (Supplementary Material S4: Figure S15).

Overall, the concurrent increases in $\bar{a}^*$ and $\bar{b}^*$ following the two episodes of survival selection against residence generated substantial increases in the mean standardized liability expectation $\bar{\eta}^*$ (Figure 6C), which in turn translated into increases in the expected phenotypic proportion of migrants versus residents $\bar{\psi}$ (Figure 6D). Due to the relative proximity to the threshold, changes in $\bar{\eta}^*$ translated almost linearly to changes in $\bar{\psi}$ and primarily reflected within-year winter progression and between-year variation in $\bar{b}^*$ rather than variation in $\bar{a}^*$ (Figure 6).

Discussion

Understanding population responses to environmentally-induced selection requires dissecting genetic and environmental components of variation in key traits; but these components become complex and entangled for phenotypically discrete traits. Our explicit decompositions of liability-scale and phenotypic-scale variation in the ecologically critical trait of seasonal migration versus residence demonstrate non-negligible additive genetic variance in liability and show how this variation is manifested phenotypically, both independently and in interaction with permanent and temporary environmental effects. Our results reveal the potential for both rapid micro-evolutionary change and phenotypic inertia in migration versus residence, as manifested in response to observed episodes of strong survival selection. This highlights the intrinsic emergence of complex interactions between micro-evolution and environmental variation in dichotomous threshold traits.

Multiscale variance partitioning and micro-evolutionary potential

Our application of a novel multistate CRAM to full-annual-cycle field observations revealed nontrivial additive genetic variation in liability for migration in a

wild partially migratory population, implying potential for micro-evolutionary responses to selection. In principle, the nonlinear genotype–phenotype map of threshold traits implies that liability-scale additive genetic variation could become partly nonadditive on the phenotypic scale on which selection directly acts (de Villemereuil et al., 2016; Dempster & Lerner, 1950). Intrinsic genetic interactions can therefore emerge and hide heritable liability-scale variation, generating "cryptic" genetic variation which is apparently shielded from direct phenotypic selection (McGuigan & Sgrò, 2009; Moorad & Linksvayer, 2008; Pulido, 2011; Roff, 1996, 1998). Yet, for threshold traits in constant environments, yielding constant fitness differences between the alternative phenotypes, the proportion of genetic variation that is cryptic is greater, and selection on genetic variation weaker, when the frequency of the commonest phenotype is higher (Falconer & Mackay, 1996; Moorad & Linksvayer, 2008; Roff, 1998). In our system, where frequencies of migration versus residence are close to parity (especially in winter occasions 2–4; Figure 5), most additive genetic variance estimated on the liability scale is phenotypically expressed. Accordingly, any selection acting on the migrant versus resident phenotypes should generate maximum selection intensity on liability, and maximum potential magnitude of micro-evolutionary response.

However, our multiscale decompositions also highlight that intrinsic gene-by-environment interactions can arise in threshold traits, which has not previously been fully considered (Reid & Acker, 2022). We show that much of the total phenotypic variance in migration versus residence results from interactions among additive liability-scale components, notably from a three-way interaction involving permanent individual and temporary environmental effects alongside additive genetic effects (Figure 5). This interaction emerges even though our current CRAM did not explicitly consider any gene-by-environment interactions in liability, as could be conceptualized through reaction norms of liability-scale plasticity. Instead, the phenotypic-scale interactions result from variation in total individual effects on liability, which generate among-individual variation in the degree and direction of labile phenotypic plasticity caused by temporary environmental deviations (Figure 1; Acker et al., 2023; Reid & Acker, 2022). Such phenotypic plasticity may then be subject to selection, for example resulting from induced costs of phenotypic change, or benefits of rapid phenotype–environment matching (Auld et al., 2010; DeWitt et al., 1998). Indeed, we previously demonstrated episodes of selection on phenotypic plasticity in migration versus residence (manifested as within-winter switching) in shags (Acker et al., 2023; Reid et al., 2020). Major discrepancies in the form and/or magnitude of selection on liabilities, and hence in micro-evolutionary responses, could therefore arise compared to expectations from existing threshold-trait theory that only considers the relative frequencies and fitness of current alternative phenotypes (de Villemereuil et al., 2016; Falconer & Mackay, 1996; Roff, 1996, 1998). Meanwhile, the joint multiscale variation in liability and phenotypic plasticity in threshold traits also implies fundamentally different evolutionary dynamics of plasticity than expected for continuous traits where reaction norms directly act on observed phenotypic scales (Lande, 2009; Nussey et al., 2007; Reid & Acker, 2022).

Moreover, permanent individual variance was the largest component of variance in liability for migration in shags (Figure 4, Table 1), causing substantial phenotypic variance in isolation and through interactions (Figure 6). This variance component encompasses nonadditive genetic effects acting on the liability scale and/or lasting effects of early-life environments that induce repeatable among-individual variation (Beldade et al., 2011; Kruuk, 2004; Scheiner, 1993). Variation in biotic or abiotic early-life conditions could therefore be one main determinant of population distributions of liabilities and resulting proportions of migrants versus residents, hence defining the extent of adult labile phenotypic plasticity and setting the stage for survival selection to further shape distributions of liabilities (Figure 1; Reid & Acker, 2022). Plastic development could thereby fundamentally shape the combined potential for subsequent labile plastic and micro-evolutionary responses to environmental perturbations and changes, shaping individual and population capacities to buffer environmental impacts (Beaman et al., 2016).

Micro-evolutionary potential in partial migration and threshold traits

Despite the key role that rapid phenotypic change in migration versus residence could play in driving spatio-seasonal eco-evolutionary dynamics in diverse animals (Hsiung et al., 2018; Pulido, 2011; Reid et al., 2018), few studies have explicitly quantified key components of genetic and environmental variation. Moreover, standardized measurement of evolutionary potential is particularly challenging for threshold traits, impeding cross-study comparisons. "Evolvability," defined as the mean-scaled additive genetic variance (Hansen & Pélabon, 2021; Hansen et al., 2011; Houle, 1992), is meaningless on the liability scale, because values are arbitrarily measured as deviations from the threshold, and additive genetic variance is only estimable relative to environmental variance. We are thus left with heritability as a standardized measure of additive genetic variation, which may primarily reflect the magnitude of environmental variance, and hence have little value for comparing evolutionary potential (Hansen & Pélabon, 2021; Hansen et al., 2011; Houle, 1992). Arbitrarily high heritabilities can be expected in studies conducted under controlled laboratory conditions or across short time periods with greatly restricted environmental variation.

Indeed, the few previous studies that quantified additive genetic variance in liability for migration versus residence reported ~50% heritability, contrasting with our 9% (Table 1). One study of brook trout (*Salvelinus fontinalis*) included only three years with two cohorts overlapping in one year (Thériault et al., 2007), and two others used captive bred and raised Atlantic salmon (*Salmo salar*; Debes et al., 2020; Páez et al., 2011). Similarly high heritabilities of proxies of seasonal migration were reported by other studies conducted under controlled captive conditions (e.g., body size, body mass, or age at maturation in salmonids: Dodson et al., 2013; migratory activity in blackcaps, *Sylvia atricapilla*: Berthold & Pulido, 1994; Pulido et al., 1996) and for threshold traits in general (Roff, 1996). Moreover, most such previous studies focused on threshold traits where phenotypic expression is (approximately) fixed, and hence not subject to temporary environmental variance. Meanwhile, relatively small heritabilities have been reported in other labile threshold traits (e.g., survival, Krebs & Loeschcke, 1997; Papaïx et al., 2010; Gauzere et al., 2020; divorce, Germain et al., 2018). Our analytical and conceptual advances, which allow estimation and interpretation of variances underlying threshold traits from incomplete observations, should now

facilitate new evaluations of components of liability-scale and phenotypic-scale variation in migration, and other traits, in wild populations.

Temporal dynamics and response to selection

Our dissection of the temporal dynamics of liabilities underlying migration versus residence reveals how phenotypic changes can emerge within and across full annual cycles. Notably, our analyses show detectable increases in mean breeding values following two known episodes of strong phenotypic survival selection against residence associated with ECEs in late-winter 2012–2013 and 2017–2018 (Figure 6A). Furthermore, these estimated micro-evolutionary responses are likely conservative, since our calculations partly assumed that dichotomous migrant versus resident phenotypes are the sole cause of selection on liability-scale breeding values (Supplementary Material S3). In fact, there could be stronger directional selection along the phenological continuum of phenotypes ranging from full-winter residence to full-winter migration which partly reflects additive genetic variation in liability (Acker et al., 2023). More generally, selection on liability could take subtler forms than the simple direct selection on dichotomous phenotype that our CRAM currently assumes (including disruptive or stabilizing selection; Acker et al., 2023; Reid & Acker, 2022). The indications that ECE-induced selection caused immediate micro-evolutionary shifts in mean liability-scale breeding values for migration that are large enough to be evident between consecutive seasonal timesteps in a wild population are therefore remarkable. In contrast, other individual-based wild population studies have commonly struggled to uncover (cross-generational) micro-evolutionary changes in traits that apparently experience directional selection spanning several years or decades (e.g., Biquet et al. , 2022; Bonnet et al., 2019; Gienapp et al., 2006; Hunter et al., 2022).

Nonetheless, the changes in population mean breeding values following the ECEs were dwarfed by simultaneous changes in mean permanent individual effects (Figure 6A and B, which may also be conservative estimates). Increases in phenotypic expression of migration versus residence following the ECEs therefore primarily reflect selection on permanent individual effects within the focal adult population rather than on additive genetic effects. Yet, the phenotypic inertia in increased migration that might be expected following such strong selection on permanent individual values in a relatively long-lived species (mean annual adult survival probability: ~0.86, Frederiksen et al., 2008, giving an expected adult lifespan of ~7 years) was not fully observed. Rather, mean permanent individual effects, and to some degree mean breeding values, decreased between the two ECEs, decreasing the expected degree of migration.

These decreases predominantly reflect effects of cohorts of new recruits that joined the focal adult population each year (Supplementary Material S4). Since individuals recruiting following the ECEs hatched some years previously (median age of first reproduction: 3 years), they cause reversion towards mean breeding values of previous adults. This reversion could be accelerated by known reproductive selection against migrants (Acker et al., 2021a; Grist et al., 2017), and potentially also by selection on prerecruitment migration versus residence. Meanwhile, among-cohort variation in mean permanent individual effects on liability likely reflects lasting effects of developmental conditions rather than substantial shifts in nonadditive genetic effects. These outcomes again point towards overarching effects of early-life conditions, not only in shaping emerging gene-by-environment interactions (outlined above), but also in shaping the phenotypic dynamics of seasonally mobile populations in response to selective ECEs.

Future prospects

High adult phenotypic repeatability of seasonal migration versus residence is increasingly observed in wild populations of diverse taxa (e.g., Kerr et al., 2009; Grist et al., 2014; Zúñiga et al., 2017; Lehnert et al., 2018; Sawyer et al., 2019). While such among-individual variation has not previously been explicitly partitioned into additive genetic versus permanent individual effects on liability- or phenotypic-scales, there is clearly scope for similar effects as uncovered in our study to act much more widely. The likely prominent role of permanent environmental effects should now drive new focus on early-life development of migration versus residence, encompassing advanced quantifications of multidimensional liability-scale reaction norms and their genetic basis and phenotypic-scale consequences. Such work can in future be facilitated by linking our conceptual and analytical framework with tracking technologies deployed on numerous related individuals, thereby integrating advances in movement ecology (Flack et al., 2022) with evolutionary quantitative genetics.

Meanwhile, our study highlights the limits of established quantitative genetic models that envisage current phenotypes as the sole substrate of selection on threshold traits (e.g., de Villemereuil et al., 2016; Roff, 1998). By focusing solely on the fitness differential between the two phenotypes, such approaches filter out liability-scale covariance between relative fitness and breeding value that defines micro-evolutionary change. Fully predicting phenotypic responses in key threshold traits, such as migration versus residence, will therefore require quantifying selection on liability that would be hidden on the dichotomous phenotypic scale (Supplementary Material S3: Figure S11). Such analyses could integrate fitness consequences of intrinsic phenotypic plasticity resulting from liability variation, including induced costs (Auld et al., 2010; DeWitt et al., 1998), alongside carry-over effects of previous phenotypic expression (Harrison et al., 2011), and indirect selection acting through other correlated traits (Lande & Arnold, 1983). These analyses will be very challenging but are in principle achievable by extending our CRAM approach to jointly estimate environmental and additive genetic covariances between liability and fitness components, following principles of multivariate animal models (Morrissey et al., 2010, 2012; Stinchcombe et al., 2014). This approach could potentially be combined with frameworks for quantifying sequential and conditional expression of fitness components (e.g., aster models, Geyer et al., 2013; de Villemereuil, 2018). Our current assumptions of constant liability-scale genetic variance across seasonal occasions, environmental conditions and sexes could be relaxed given more years of phenotypic and pedigree data, likely revealing further drivers and constraints on system dynamics. Yet, our current analyses provide the first insights into the fundamental quantitative genetic basis for joint plastic and evolutionary rescue of partially migratory populations experiencing changing circannual environments.

Supplementary material

Supplementary material is available online at *Evolution*.

Data availability

All data and code used in this study are available from Dryad at https://doi.org/10.5061/dryad.pk0p2ngtg.

Author contributions

P.A. and J.M.R. formulated the ideas and conceptual developments. J.M.R. and F.D. conceived the migration field study. F.D. and S.W. conceived the field study to generate pedigree data. F.D., S.W., M.P.H., M.A.N., S.J.B., R.L.S., C.G., T.I.M., and J.M.R. organized and undertook long-term field data collection. P.A. devised the quantitative methodology, coded the models, analyzed the data, and drafted the manuscript, assisted by J.M.R.. All authors contributed to manuscript editing.

Conflict of interest: The authors declare no conflict of interest.

Acknowledgments

We thank everyone who contributed to long-term field data collection, particularly Raymond Duncan, Sarah Fenn, Hannah Grist, Calum Scott, Jenny Sturgeon, Moray Souter, John Anderson, and Harry Bell; and thank NatureScot for allowing work on the Isle of May National Nature Reserve, and Isle of May Bird Observatory Trust for supporting the long-term ringing of shags. We thank Stefanie Muff for helpful discussions, and Rita Fortuna and Thomas R. Haaland for useful comments on a manuscript draft. The current study was funded by Natural Environment Research Council (NERC; awards NE/M005186/1, NE/R000859/1, and NE/R016429/1 as part of the UK-SCaPE program delivering National Capability), Norwegian Research Council (SFF-III grant 223257, FRIPRO grant 313570), NTNU and University of Aberdeen. Analyses were performed using the IDUN cluster of NTNU.

References

Acker, P., Burthe, S. J., Newell, M. A., Grist, H., Gunn, C., Harris, M. P., Payo-Payo, A., Wanless, S., Swann, R. L., Daunt, F., & Reid, J. M. (2021a). Episodes of opposing survival and reproductive selection cause strong fluctuating selection on seasonal migration versus residence. *Proceedings of the Royal Society of London. Series B*, *288*, 20210404. https://doi.org/10.1098/rspb.2021.0404

Acker, P., Daunt, F., Wanless, S., Burthe, S. J., Newell, M. A., Harris, M. P., Grist, H., Sturgeon, J., Swann, R. L., Gunn, C., Payo-Payo, A., & Reid, J. M. (2021b). Strong survival selection on seasonal migration versus residence induced by extreme climatic events. *Journal of Animal Ecology*, *90*(4), 796–808. https://doi.org/10.1111/1365-2656.13410

Acker, P., Daunt, F., Wanless, S., Burthe, S. J., Newell, M. A., Harris, M. P., Gunn, C., Swann, R. L., Payo-Payo, A., & Reid, J. M. (2023). Hierarchical variation in phenotypic flexibility across timescales and associated survival selection shape the dynamics of partial seasonal migration. *American Naturalist*, *201*(2), 269–286. https://doi.org/10.1086/722484

Auld, J. R., Agrawal, A. A., & Relyea, R. A. (2010). Re-evaluating the costs and limits of adaptive phenotypic plasticity. *Proceedings of the Royal Society of London. Series B*, *277*, 503–511. https://doi.org/10.1098/rspb.2009.1355

Bay, R. A., Rose, N., Barrett, R., Bernatchez, L., Ghalambor, C. K., Lasky, J. R., Brem, R. B., Palumbi, S. R., & Ralph, P. (2017). Predicting responses to contemporary environmental change using evolutionary response architectures. *American Naturalist*, *189*(5), 463–473. https://doi.org/10.1086/691233

Beaman, J. E., White, C. R., & Seebacher, F. (2016). Evolution of plasticity: Mechanistic link between development and reversible acclimation. *Trends in Ecology and Evolution*, *31*(3), 237–249. https://doi.org/10.1016/j.tree.2016.01.004

Beldade, P., Mateus, A. R. A., & Keller, R. A. (2011). Evolution and molecular mechanisms of adaptive developmental plasticity. *Molecular Ecology*, *20*, 1347–1363. https://doi.org/10.1111/j.1365-294X.2011.05016.x

Berg, J. E., Hebblewhite, M., c. St. Clair, C., & Merrill, E. H. (2019). Prevalence and mechanisms of partial migration in ungulates. *Frontiers in Ecology and Evolution*, *7*, 325. https://doi.org/10.3389/fevo.2019.00325

Berthold, P. (1988). Evolutionary aspects of migratory behaviour in European warblers. *Journal of Evolutionary Biology*, *1*(3), 195–209. https://doi.org/10.1046/j.1420-9101.1998.1030195.x

Berthold, P., & Pulido, F. (1994). Heritability of migratory activity in a natural bird population. *Proceedings of the Royal Society of London. Series B*, *257*, 311–315. https://doi.org/10.1098/rspb.1994.0131

Biquet, J., Bonamour, S., De Villemereuil, P., De Franceschi, C., & Teplitsky, C. (2022). Phenotypic plasticity drives phenological changes in a Mediterranean blue tit population. *Journal of Evolutionary Biology*, *35*(2), 347–359. https://doi.org/10.1111/jeb.13950

Biro, P. A., & Dingemanse, N. J. (2009). Sampling bias resulting from animal personality. *Trends in Ecology and Evolution*, *24*(2), 66–67. https://doi.org/10.1016/j.tree.2008.11.001

Bonnet, T., Morrissey, M. B., Morris, A., Morris, S., Clutton-Brock, T. H., Pemberton, J. M., & Kruuk, L. E. B. (2019). The role of selection and evolution in changing parturition date in a red deer population. *PLoS Biology*, *17*(11), e3000493. https://doi.org/10.1371/journal.pbio.3000493

Bossu, C. M., Heath, J. A., Kaltenecker, G. S., Helm, B., & Ruegg, K. C. (2022). Clock-linked genes underlie seasonal migratory timing in a diurnal raptor. *Proceedings of the Royal Society of London. Series B*, *289*, 20212507. https://doi.org/10.1098/rspb.2021.2507

Boyle, W. A., Norris, D. R., & Guglielmo, C. G. (2010). Storms drive altitudinal migration in a tropical bird. *Proceedings of the Royal Society B: Biological Sciences*, *277*(1693), 2511–2519. https://doi.org/10.1098/rspb.2010.0344

Brodersen, J., Nilsson, P. A., Hansson, L. -A., Skov, C., & Brönmark, C. (2008). Condition-dependent individual decision-making determines cyprinid partial migration. *Ecology*, *89*(5), 1195–1200. https://doi.org/10.1890/07-1318.1

Brodersen, J., Chapman, B. B., Nilsson, P. A., Skov, C., Hansson, L. A., & Brönmark, C. (2014). Fixed and flexible: coexistence of obligate and facultative migratory strategies in a freshwater fish. *PLoS One*, *9*(3), e90294. https://doi.org/10.1371/journal.pone.0090294

Buchan, C., Gilroy, J. J., Catry, I., & Franco, A. M. A. (2020). Fitness consequences of different migratory strategies in partially migratory populations: A multi-taxa meta-analysis. *Journal of Animal Ecology*, *89*(3), 678–690. https://doi.org/10.1111/1365-2656.13155

Cagnacci, F., Focardi, S., Heurich, M., Stache, A., Hewison, A. J. M., Morellet, N., Kjellander, P., Kjellander, P., Linnell, J. D. C., Mysterud, A., Neteler, M., Delucchi, L., Ossi, F., & Urbano, F. (2011). Partial migration in roe deer: Migratory and resident tactics are end points of a behavioural gradient determined by ecological factors. *Oikos*, *120*, 1790–1802. https://doi.org/10.1111/j.1600-0706.2011.19441.x

Carpenter, B., Gelman, A., Hoffman, M. D., Lee, D., Goodrich, B., Betancourt, M., Brubaker, M., Guo, J., Li, P., & Riddell, A. (2017). Stan: A probabilistic programming language. *Journal of Statistical Software*, *76*(1), 1–32. https://doi.org/10.18637/jss.v076.i01

Caswell, H. (2001). *Matrix population models*. Sinauer.

Chapman, B. B., Hulthen, K., Brodersen, J., Nilsson, P. A., Skov, C., Hansson, L. A., & Brönmark, C. (2012). Partial migration in fishes: Causes and consequences. *Journal of Fish Biology*, *81*(2), 456–478. https://doi.org/10.1111/j.1095-8649.2012.03342.x

Chevin, L. M., Leung, C., L.e. Rouzic, A., & Uller, T. (2022). Using phenotypic plasticity to understand the structure and evolution of the genotype–phenotype map. *Genetica*, *150*(3-4), 209–221. https://doi.org/10.1007/s10709-021-00135-5

Daunt, F., Reed, T. E., Newell, M., Burthe, S., Phillips, R. A., Lewis, S., & Wanless, S. (2014). Longitudinal bio-logging reveals interplay between extrinsic and intrinsic carry-over effects in a long-lived vertebrate. *Ecology*, *95*(8), 2077–2083. https://doi.org/10.1890/13-1797.1

de Villemereuil, P. (2018). Quantitative genetic methods depending on the nature of the phenotypic trait. *Annals of the New York Academy of Sciences*, *1422*, 29–47. https://doi.org/10.1111/nyas.13571

de Villemereuil, P., Schielzeth, H., Nakagawa, S., & Morrissey, M. (2016). General methods for evolutionary quantitative genetic inference from generalized mixed models. *Genetics*, *204*(3), 1281–1294. https://doi.org/10.1534/genetics.115.186536

Debes, P. V., Piavchenko, N., Erkinaro, J., & Primmer, C. R. (2020). Genetic growth potential, rather than phenotypic size, predicts migration phenotype in Atlantic salmon. *Proceedings of the Royal Society of London. Series B*, *287*, 20200867. https://doi.org/10.1098/rspb.2020.0867

Dempster, E. R., & Lerner, I. M. (1950). Heritability of threshold characters. *Genetics*, *35*(2), 212–236. https://doi.org/10.1093/genetics/35.2.212

DeWitt, T. J., Sih, A., & Wilson, D. S. (1998). Costs and limits of phenotypic plasticity. *Trends in Ecology and Evolution*, *13*(2), 77–81. https://doi.org/10.1016/s0169-5347(97)01274-3

Dodson, J. J., Aubin-Horth, N., Thériault, V., & Páez, D. J. (2013). The evolutionary ecology of alternative migratory tactics in salmonid fishes. *Biological Review*, *88*, 602–625. https://doi.org/10.1111/brv.12019

Eggeman, S. L., Hebblewhite, M., Bohm, H., Whittington, J., & Merrill, E. H. (2016). Behavioural flexibility in migratory behaviour in a long-lived large herbivore. *Journal of Animal Ecology*, *85*(3), 785–797. https://doi.org/10.1111/1365-2656.12495

Falconer, D. S., & Mackay, T. (1996). *Introduction to quantitative genetics* (4th ed.). Pearson.

Flack, A., Aikens, E. O., A. Kölzsch, A. K., Nourani, E., Snell, K. R. S., Fiedler, W., Linek, N., Bauer, H. -G., Thorup, K., Partecke, J., Wikelski, M., & Williams, H. J. (2022). New frontiers in bird migration research. *Current Biology*, *32*, R1187–R1199. https://doi.org/10.1016/j.cub.2022.08.028

Frederiksen, M., Daunt, F., Harris, M. P., & Wanless, S. (2008). The demographic impact of extreme events: Stochastic weather drives survival and population dynamics in a long-lived seabird. *Journal of Animal Ecology*, *77*(5), 1020–1029. https://doi.org/10.1111/j.1365-2656.2008.01422.x

Fudickar, A. M., Schmidt, A., Hau, M., Quetting, M., & Partecke, J. (2013). Female-biased obligate strategies in a partially migratory population. *Journal of Animal Ecology*, *82*(4), 863–871. https://doi.org/10.1111/1365-2656.12052

Gauzere, J., Pemberton, J. M., Morris, S., Morris, A., Kruuk, L. E., & Walling, C. A. (2020). The genetic architecture of maternal effects across ontogeny in the red deer. *Evolution*, *74*, 1378–1391. https://doi.org/10.1111/evo.14000

Gelman, A., Meng, X. -L., & Stern, H. (1996). Posterior predictive assessment of model fitness via realized discrepancies. *Statistica Sinica*, *6*, 733–760.

Germain, R. R., Wolak, M. E., & Reid, J. M. (2018). Individual repeatability and heritability of divorce in a wild population. Biol. Let. *14*, 20180061. https://doi.org/10.1098/rsbl.2018.0061

Geyer, C. J., Ridley, C. E., Latta, R. G., Etterson, J. R., & Shaw, R. G. (2013). Local adaptation and genetic effects on fitness: Calculations for exponential family models with random effects. *Annals of Applied Statistics*, *7*, 1778–1795. https://doi.org/10.1214/13-AOAS653

Gianola, D. (1982). Theory and analysis of threshold characters. *Journal of Animal Science*, *54*(5), 1079–1096. https://doi.org/10.2527/jas1982.5451079x

Gienapp, P., Postma, E., & Visser, M. E. (2006). Why breeding time has not responded to selection for earlier breeding in a songbird population. *Evolution*, *60*, 2381–2388. https://doi.org/10.1111/j.0014-3820.2006.tb01872.x

Gienapp, P., Teplitsky, C., Alho, J. S., Mills, J. A., & Merilä, J. (2008). Climate change and evolution: Disentangling environmental and genetic responses. *Molecular Ecology*, *17*, 167–178. https://doi.org/10.1111/j.1365-294X.2007.03413.x

Gimenez, O., Viallefont, A., Charmantier, A., Pradel, R., Cam, E., Brown, C. R., Anderson, M. D., Bomberger Brown, M., Covas, R., & Gaillard, J. -M. (2008). The risk of flawed inference in evolutionary studies when detectability is less than one. *American Naturalist*, *172*, 441–448. https://doi.org/10.1086/589520

Grayson, K. L., Bailey, L. L., & Wilbur, H. M. (2011). Life history benefits of residency in a partially migrating pond-breeding amphibian. *Ecology*, *92*, 1236–1246. https://doi.org/10.1890/11-0133.1

Grist, H., Daunt, F., Wanless, S., Burthe, S. J., Newell, M. A., Harris, M. P., & Reid, J. M. (2017). Reproductive performance of resident and migrant males, females and pairs in a partially migratory bird. *Journal of Animal Ecology*, *86*(5), 1010–1021. https://doi.org/10.1111/1365-2656.12691

Grist, H., Daunt, F., Wanless, S., Nelson, E. J., Harris, M. P., Newell, M., Burthe, S., & Reid, J. M. (2014). Site fidelity and individual variation in winter location in partially migratory European shags. *PLoS One*, *9*(6), e98562. https://doi.org/10.1371/journal.pone.0098562

Hadfield, J. D. (2008). Estimating evolutionary parameters when viability selection is operating. *Proceedings of the Royal Society of London. Series B*, *275*(1635), 723–734. https://doi.org/10.1098/rspb.2007.1013

Hadfield, J. D., Wilson, A. J., Garant, D., Sheldon, B. C., & Kruuk, L. E. B. (2010). The misuse of BLUP in ecology and evolution. *American Naturalist*, *175*, 116–125. https://doi.org/10.1086/648604

Hansen, T. F., & Pélabon, C. (2021). Evolvability: A quantitative-genetics perspective. *Annual Review of Ecology, Evolution, and Systematics*, *52*, 153–175. https://doi.org/10.1146/annurev-ecolsys-011121-021241

Hansen, T. F., Pélabon, C., & Houle, D. (2011). Heritability is not evolvability. *Evolutionary Biology*, *38*, 258–277. https://doi.org/10.1007/s11692-011-9127-6

Harrison, X. A., Blount, J. D., Inger, R., Norris, D. R., & Bearhop, S. (2011). Carry-over effects as drivers of fitness differences in animals. *Journal of Animal Ecology*, *80*(1), 4–18. https://doi.org/10.1111/j.1365-2656.2010.01740.x

Hegemann, A., Marra, P. P., & Tieleman, B. I. (2015). Causes and consequences of partial migration in a passerine bird. *American Naturalist*, *186*, 531–546. https://doi.org/10.1086/682667

Houle, D. (1992). Comparing evolvability and variability of quantitative traits. *Genetics*, *130*(1), 195–204. https://doi.org/10.1093/genetics/130.1.195

Houle, D., Govindaraju, D. R., & Omholt, S. (2010). Phenomics: The next challenge. *Nature Reviews Genetics*, *11*, 855. https://doi.org/10.1038/nrg2897

Hsiung, A. C., Boyle, W. A., Cooper, R. J., & Chandler, R. B. (2018). Altitudinal migration: Ecological drivers, knowledge gaps, and conservation implications. *Biological Review*, *93*, 2049–2070. https://doi.org/10.1111/brv.12435

Hunter, D. C., Ashraf, B., Bérénos, C., Ellis, P. A., Johnston, S. E., Wilson, A. J., Pilkington, J. G., Pemberton, J. M., & Slate, J. (2022). Using genomic prediction to detect microevolutionary change of a quantitative trait. *Proceedings of the Royal Society of London. Series B*, *289*, 20220330. https://doi.org/10.1098/rspb.2022.0330

Husby, A., Nussey, D. H., Visser, M. E., Wilson, A. J., Sheldon, B. C., & Kruuk, L. E. B. (2010). Contrasting patterns of phenotypic plasticity in reproductive traits in two great tit (*Parus major*) populations. *Evolution*, *64*, 2221–2237. https://doi.org/10.1111/j.1558-5646.2010.00991.x

Keogan, K., Lewis, S., Howells, R. J., Newell, M. A., Harris, M. P., Burthe, S., Phillips, R. A., Wanless, S., Phillimore, A. B., & Daunt, F. (2021). No evidence for fitness signatures consistent with increasing trophic mismatch over 30 years in a population of European shag *Phalacrocorax aristotelis*. *Journal of Animal Ecology*, *90*(2), 432–446. https://doi.org/10.1111/1365-2656.13376

Kerr, L. A., Secor, D. H., & Piccoli, P. M. (2009). Partial migration of fishes as exemplified by the estuarine-dependent white perch. *Fisheries*, *34*, 114–123. http://doi.org/10.1577/1548-8446-34.3.114

Kingsolver, J. G., & Buckley, L. B. (2017). Evolution of plasticity and adaptive responses to climate change along climate gradients. *Proceedings of the Royal Society of London. Series B, Biological Sciences*, *284*(1860), 20170386. https://doi.org/10.1098/rspb.2017.0386

Krebs, R. A., & Loeschcke, V. (1997). Estimating heritability in a threshold trait: Heat-shock tolerance in *Drosophila buzzatii*. *Heredity*, *79*(3), 252–259. https://doi.org/10.1038/sj.hdy.6882000

Kruuk, L. E. B. (2004). Estimating genetic parameters in natural populations using the "animal model." *Philosophical Transactions of the Royal Society B*, *359*, 873–890. https://doi.org/10.1098/rstb.2003.1437

Lande, R. (2009). Adaptation to an extraordinary environment by evolution of phenotypic plasticity and genetic assimilation. *Journal of Evolutionary Biology*, *22*(7), 1435–1446. https://doi.org/10.1111/j.1420-9101.2009.01754.x

Lande, R., & Arnold, S. (1983). The measurement of selection on correlated characters. *Evolution*, *37*, 1210–1226. https://doi.org/10.1111/j.1558-5646.1983.tb00236.x

Lebreton, J. D., Burnham, K. P., Clobert, J., & Anderson, D. R. (1992). Modeling survival and testing biological hypotheses using marked animals: A unified approach with case studies. *Ecological Monographs*, *62*, 67–118. https://doi.org/10.2307/2937171

Lebreton, J. -D., & Pradel, R. (2002). Multistate recapture models: Modelling incomplete individual histories. *Journal of Applied Statistics*, *29*, 353–369. https://doi.org/10.1080/02664760120108638

Lehnert, L. S., Kramer-Schadt, S., Teige, T., Hoffmeister, U., Popa-Lisseanu, A., Bontadina, F., Ciechanowski, M., Dechmann, D. K. N., Kravchenko, L., Presetnik, P., & Starrach, M. (2018). Variability and repeatability of noctule bat migration in Central Europe: Evidence for partial and differential migration. *Proceedings of the Royal Society of London. Series B*, *285*, 20182174. https://doi.org/10.1098/rspb.2018.2174

Lemopoulos, A. S., Uusi-Heikkilä, P., Hyvärinin, N., Alioravainen, J., Prokkola, C., Elvidge, A. V., & Vainikka, A. (2019). Association mapping based on a common-garden migration experiment reveals candidate genes for migration tendency in brown trout. *G3: Genes, Genomes, Genetics*, *9*, 2887–2896. https://doi.org/10.1534/g3.119.400369

McGuigan, K., & Sgrò, C. M. (2009). Evolutionary consequences of cryptic genetic variation. *Trends in Ecology and Evolution*, *24*(6), 305–311. https://doi.org/10.1016/j.tree.2009.02.001

Merilä, J., & Hendry, A. P. (2014). Climate change, adaptation, and phenotypic plasticity: The problem and the evidence. *Evolutionary Applications*, *7*(1), 1–14. https://doi.org/10.1111/eva.12137

Moorad, J. A., & Linksvayer, T. A. (2008). Levels of selection on threshold characters. *Genetics*, *179*(2), 899–905. https://doi.org/10.1534/genetics.108.086959

Moorad, J. A., & Promislow, D. E. L. (2011). Evolutionary demography and quantitative genetics: Age-specific survival as a threshold trait. *Proceedings of the Royal Society of London. Series B*, *278*, 144–151. https://doi.org/10.1098/rspb.2010.0992

Morrissey, M. B. (2015). Evolutionary quantitative genetics of nonlinear developmental systems. *Evolution*, *69*(8), 2050–2066. https://doi.org/10.1111/evo.12728

Morrissey, M. B., de Villemereuil, P., Doligez, B., & Gimenez, O. (2014). Bayesian approaches to the quantitative genetic analysis of natural populations. In A. Charmantier, D. Garant, & L. E. B. Kruuk (Eds.), *Quantitative genetics in the wild* (pp. 228–253). Oxford University Press. https://doi.org/10.1093/acprof:oso/9780199674237.003.0014

Morrissey, M. B., Kruuk, L. E. B., & Wilson, A. J. (2010). The danger of applying the breeder's equation in observational studies of natural populations. *Journal of Evolutionary Biology*, *23*, 2277–2288. https://doi.org/10.1111/j.1420-9101.2010.02084.x

Morrissey, M. B., Parker, D. J., Korsten, P., Pemberton, J. M., Kruuk, L. E. B., & Wilson, A. J. (2012). The prediction of adaptive evolution: Empirical application of the secondary theorem of selection and comparison to the breeder's equation. *Evolution*, *66*, 2399–2410. https://doi.org/10.1111/j.1558-5646.2012.01632.x

Nakagawa, S., & Freckleton, R. P. (2008). Missing inaction: The dangers of ignoring missing data. *Trends in Ecology and Evolution*, *23*(11), 592–596. https://doi.org/10.1016/j.tree.2008.06.014

Nelder, J. A., & Wedderburn, R. W. (1972). Generalized linear models. *Journal of the Royal Statistical* Society, *Series A*, *135*, 370–384. https://doi.org/10.2307/2344614

Nussey, D. H., Wilson, A. J., & Brommer, J. E. (2007). The evolutionary ecology of individual phenotypic plasticity in wild populations. *Journal of Evolutionary Biology*, *20*, 831–844. https://doi.org/10.1111/j.1420-9101.2007.01300.x

Páez, D. J., Brisson-Bonenfant, C., Rossignol, O., Guderley, H. E., Bernatchez, L., & Dodson, J. J. (2011). Alternative developmental pathways and the propensity to migrate: A case study in the Atlantic salmon. *Journal of Evolutionary Biology*, *24*(2), 245–255. https://doi.org/10.1111/j.1420-9101.2010.02159.x

Papaïx, J., Cubaynes, S., Buoro, M., Charmantier, A., Perret, P., & Gimenez, O. (2010). Combining capture-recapture data and pedigree information to assess heritability of demographic parameters in the wild. *Journal of Evolutionary Biology*, *23*(10), 2176–2184. https://doi.org/10.1111/j.1420-9101.2010.02079.x

Pedersen, S., Berg, P. R., Culling, M., Danzmann, R. G., Glebe, B., Leadbeater, S., Liens, S., Moen, T., Vandersteen, W., & Boulding, E. G. (2013). Quantitative trait loci for precocious parr maturation, early smoltification, and adult maturation in double-backcrossed trans-Atlantic salmon (*Salmo salar*). *Aquaculture*, *410*(-411), 164–171. https://doi.org/10.1016/j.aquaculture.2013.06.039

Pigeon, G., Ezard, T. H., Festa-Bianchet, M., Coltman, D. W., & Pelletier, F. (2017). Fluctuating effects of genetic and plastic changes in body mass on population dynamics in a large herbivore. *Ecology*, *98*, 2456–2467. https://doi.org/10.1002/ecy.1940

Postma, E. (2006). Implications of the difference between true and predicted breeding values for the study of natural selection and micro-evolution. *Journal of Evolutionary Biology*, *19*(2), 309–320. https://doi.org/10.1111/j.1420-9101.2005.01007.x

Pulido, F. (2011). Evolutionary genetics of partial migration – the threshold model of migration revis(it)ed. *Oikos*, *120*(12), 1776–1783. https://doi.org/10.1111/j.1600-0706.2011.19844.x

Pulido, F., Berthold, P., & van Noordwijk, A. J. (1996). Frequency of migrants and migratory activity are genetically correlated in a bird population: Evolutionary implications. *Proceedings of the National Academy of Sciences*, *93*(25), 14642–14647. https://doi.org/10.1073/pnas.93.25.14642

R Core Team. (2022). *R: A language and environment for statistical computing*. R Foundation for Statistical Computing. https://doi.org/https://www.R-project.org/

Reid, J. M., & Acker, P. (2022). Properties of phenotypic plasticity in discrete threshold traits. *Evolution*, *76*(2), 190–206. https://doi.org/10.1111/evo.14408

Reid, J. M., Souter, M., Fenn, S. R., Acker, P., Payo-Payo, A., Burthe, S. J., Wanless, S., & Daunt, F. (2020). Among-individual and within-individual variation in seasonal migration covaries with subsequent reproductive success in a partially migratory bird. *Proceedings of the Royal Society of London. Series B*, *287*, 20200928. https://doi.org/10.1098/rspb.2020.0928

Reid, J. M., Travis, J. M. J., Daunt, F., Burthe, S. J., Wanless, S., & Dytham, C. (2018). Population and evolutionary dynamics in spatially structured seasonally varying environments. *Biological Review*, *93*, 1578–1603. https://doi.org/10.1111/brv.12409

Robertson, A. (1950). Heritability of threshold characters, supplementary material. *Genetics*, *35*, 234–236. https://doi.org/10.1093/genetics/35.2.212

Roff, D. A. (1996). The evolution of threshold traits in animals. *Quarterly Review of Biology*, *71*(1), 3–35. https://doi.org/10.1086/419266

Roff, D. A. (1998). Evolution of threshold traits: The balance between directional selection, drift and mutation. *Heredity*, *80*(1), 25–32. https://doi.org/10.1038/sj.hdy.6882620

Sawyer, H., Merkle, J. A., Middleton, A. D., Dwinnell, S. P. H., & Monteith, K. L. (2019). Migratory plasticity is not ubiquitous among large herbivores. *Journal of Animal Ecology*, *88*(3), 450–460. https://doi.org/10.1111/1365-2656.12926

Scheiner, S. M. (1993). Genetics and evolution of phenotypic plasticity. *Annual Review of Ecology, Evolution, and Systematics*, *24*, 35–68.

Sgrò, C. M., Terblanche, J. S., & Hoffmann, A. A. (2016). What can plasticity contribute to insect responses to climate change. *Annual Review of Entomology*, *61*, 433–451. https://doi.org/10.1146/annurev-ento-010715-023859

Sinclair-Waters, M., Ødegård, J., Korsvoll, S. A., Moen, T., Lien, S., Primmer, C. R., & Barson, N. J. (2020). Beyond large-effect loci: Large-scale GWAS reveals a mixed large-effect and polygenic architecture for age at maturity of Atlantic salmon. *Genetics, Selection, Evolution*, *52*(1), 9. https://doi.org/10.1186/s12711-020-0529-8

Stinchcombe, J. R., Simonsen, A. K., & Blows, M. W. (2014). Estimating uncertainty in multivariate responses to selection. *Evolution*, *68*(4), 1188–1196. https://doi.org/10.1111/evo.12321

Thériault, V., Garant, D., Bernatchez, L., & Dodson, J. J. (2007). Heritability of life-history tactics and genetic correlation with body size in a natural population of brook charr (*Salvelinus fontinalis*). *Journal of Evolutionary Biology*, *20*(6), 2266–2277. https://doi.org/10.1111/j.1420-9101.2007.01417.x

Wolak, M. E., & Reid, J. M. (2017). Accounting for genetic differences among unknown parents in microevolutionary studies: How to include genetic groups in quantitative genetic animal models. *Journal of Animal Ecology*, *86*(1), 7–20. https://doi.org/10.1111/1365-2656.12597

Wright, S. (1934). An analysis of variability in number of digits in an inbred strain of guinea pigs. *Genetics*, *19*(6), 506–536. https://doi.org/10.1093/genetics/19.6.506

Xu, W., Barker, K., Shawler, A., Van Scoyoc, A., Smith, J. A., Mueller, T., Sawyer, H., Andreozzi, C., Bidder, O. R., Karandikar, H., Mumme, S., Templin, E., & Middleton, A. D. (2021). The plasticity of ungulate migration in a changing world. *Ecology*, *102*(4), 1–14. https://doi.org/10.1002/ecy.3293

Yackulic, C. B., Blake, S., & Bastille-Rousseau, G. (2017). Benefits of the destinations, not costs of the journeys, shape partial migration patterns. *Journal of Animal Ecology*, *86*(4), 972–982. https://doi.org/10.1111/1365-2656.12679

Zúñiga, D., Gager, Y., Kokko, H., Fudickar, A. M., Schmidt, A., Naef-Daenzer, B., Wikelski, M., & Partecke, J. (2017). Migration confers winter survival benefits in a partially migratory songbird. *eLife*, *6*, e28123. https://doi.org/10.7554/eLife.28123